

# Tunneling of the hard-core model on finite triangular lattices

Alessandro Zocca\*

January 25, 2017

## Abstract

We consider the hard-core model on finite triangular lattices with Metropolis dynamics. Under suitable conditions on the triangular lattice dimensions, this interacting particle system has three maximum-occupancy configurations and we investigate its high-fugacity behavior by studying tunneling times, i.e., the first hitting times between these maximum-occupancy configurations, and the mixing time. The proof method relies on the analysis of the corresponding state space using geometrical and combinatorial properties of the hard-core configurations on finite triangular lattices, in combination with known results for first hitting times of Metropolis Markov chains in the equivalent zero-temperature limit. In particular, we show how the order of magnitude of the expected tunneling times depends on the triangular lattice dimensions in the low-temperature regime and prove the asymptotic exponentiality of the rescaled tunneling time leveraging the intrinsic symmetry of the state space.

*Keywords:* hard-core model; Metropolis dynamics; finite triangular lattice; tunneling time; mixing time.

## 1 Introduction

The *hard-core model* was introduced in the chemistry and statistical physics literature to describe the behavior of a gas whose particles have non-negligible radii and cannot overlap [23, 43, 47].

A finite undirected graph  $\Lambda = (V, E)$  describes the spatial structure of the finite volume in which the particles interact. More specifically, the vertices of the graph  $\Lambda$  represent the possible sites where particles can reside, while the hard-core constraints are represented by edges connecting the pairs of sites that cannot be occupied simultaneously. Particle configurations that do not violate these hard-core constraints are then in one-to-one correspondence with the independent sets of the graph  $\Lambda$ , whose collection we denote by  $\mathcal{I}(\Lambda)$ . Given  $\lambda > 0$ , the *hard-core measure with activity (or fugacity)  $\lambda$*  is the probability measure on  $\mathcal{I}(\Lambda)$  defined by

$$\pi_\lambda(I) := \frac{\lambda^{|I|}}{Z_\lambda(\Lambda)}, \quad I \in \mathcal{I}(\Lambda), \quad (1)$$

where  $Z_\lambda(\Lambda)$  is the appropriate normalizing constant, also called *partition function*.

Both physicists and mathematicians have been interested in the behavior of the hard-core model on infinite graphs, in particular the *square lattice*  $\mathbb{Z}^2$ , focusing on uniqueness/non-uniqueness phase transition as  $\lambda$  grows [3, 5, 6, 41, 42, 44, 48]. The same phenomenon has been studied also for the hard-core model on  $\mathbb{Z}^d$  [14, 18, 39] and on the *infinite triangular lattice* [1, 2, 22, 25]. This latter is also known in the literature as *hard-hexagon model*. The hard-core model on *infinite regular trees* (also known as *Cayley trees* or *Bethe lattice*) and its multistate generalization have received great attention in the applied probability literature [19, 26, 32, 40, 45, 46], as instrumental to understand the performance of certain loss networks.

In this paper we focus on the *dynamics* of particles with hard-core repulsion on *finite* graphs. The evolution over time of this interacting particle system is described by a reversible single-site update Markov chain  $\{X_t\}_{t \in \mathbb{N}}$  with Metropolis transition probabilities, parametrized by the fugacity  $\lambda \geq 1$ . More precisely, at every step a site of  $\Lambda$  is selected uniformly at random; if such a site is unoccupied, then a particle is placed there with probability 1 if and only if all the neighboring sites are also unoccupied; if instead the selected site is occupied, the particle is removed with probability  $1/\lambda$ .

Other single-site update dynamics (e.g., Glauber dynamics) for the hard-core model have received a lot of attention in the discrete mathematics community [7, 16, 17, 20, 21, 24, 31, 35], where they are instrumental to sample weighted independent sets. Aiming to understand the performance of this local Markov chain Monte Carlo method, the main focus of this literature is on *mixing times* and on how they scale in the graph size. Indeed, the behavior of these MCMC changes dramatically as the fugacity  $\lambda$  grows, going from a fast convergence to stationarity (“*fast mixing*”) to an exponentially slow one (“*slow mixing*”); this phenomenon is intimately related to the aforementioned phase transition phenomenon of the hard-core model on infinite graphs.

\*Centrum Wiskunde & Informatica, Amsterdam. Email: zocca@cwi.nl

The main focus of the present paper is on the hard-core particle dynamics  $\{X_t\}_{t \in \mathbb{N}}$  on finite graphs when the fugacity grows large, i.e.,  $\lambda \rightarrow \infty$ . In this regime, the hard-core measure (1) favors configurations with a maximum number of particles and we are interested in describing the *tunneling behavior* of such a particle system, i.e., how it evolves between these maximum-occupancy configurations. To understand the transient behavior of the hard-core model in the high-fugacity regime, we study the asymptotic behavior of the *first hitting times* of the Markov chain  $\{X_t\}_{t \in \mathbb{N}}$  between the maximum-occupancy configurations, which tell us how “rigid” they are and how long it takes for the particle system to “switch” between them.

The hard-core model has been successfully used to model certain random-access protocols for wireless networks [15, 49, 50]. In this context understanding the tunneling behavior of the hard-core model is instrumental to analyze *temporal starvation phenomena* for these communication networks and their impact on performance [53].

Tunneling phenomena of the hard-core model have already been studied on complete partite graphs [51, 52] and on square grid graphs [37]. In this work we focus on the case where  $\Lambda$  is a *finite triangular lattice*. Imposing periodic boundary conditions, there are three maximum-occupancy configurations on such graphs, as illustrated in Figure 1. These three hard-core configurations, denoted as **a**, **b**, and **c**, correspond to the natural tripartition of the graph  $\Lambda$ .

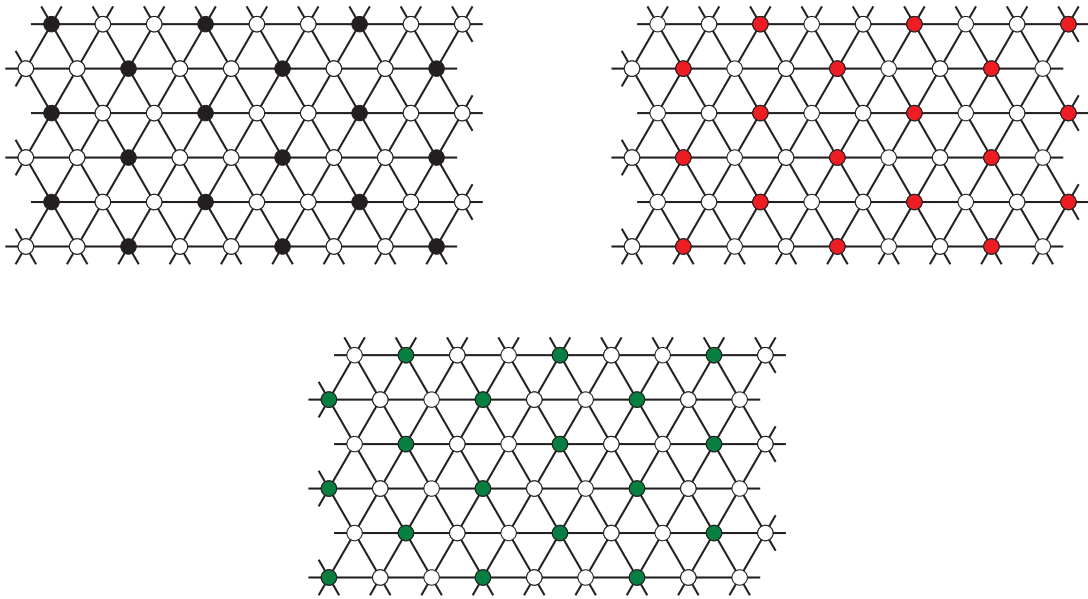


Figure 1: The three maximum-occupancy configurations **a**, **b**, and **c** on the  $6 \times 9$  triangular lattice

As the fugacity grows large, the system spends roughly one third of the time in each of these three configurations. However, it takes a long time for the Markov chain  $\{X_t\}_{t \in \mathbb{N}}$  to move from one maximum-occupancy configuration to another, since such a transition involves the occurrence of rare events. Intuitively, along any such a transition, the Markov chain  $\{X_t\}_{t \in \mathbb{N}}$  must follow a path through mixed-activity particle patterns that, having fewer particles, are highly unlikely in view of (1) and the time to reach such configurations is correspondingly long.

By introducing the *inverse temperature*  $\beta = \log \lambda$  and an appropriate Hamiltonian, the Markov chain  $\{X_t\}_{t \in \mathbb{N}}$  can be seen as a Freidlin-Wentzell Markov chain with Metropolis transition probabilities and the hard-core measure (1) rewrites as a Gibbs distribution. In this setting, the high-fugacity regime in which we are interested corresponds to the low-temperature limit  $\beta \rightarrow \infty$  and the maximum-occupancy configurations are the *stable configurations* of the system, i.e., the global minima of the Hamiltonian.

This identification allow us to use the *pathwise approach* [8, 33], a framework that has been successfully used to study metastability problem for many finite-volume models in a low-temperature regime, see e.g., [10, 11, 12, 13, 27, 36, 38]. In this paper we mostly make use of the extension of the classical pathwise approach developed in [37] that covers the case of *tunneling times*. The crucial idea behind this method is to understand which paths the Markov chain most likely follows in the low-temperature regime and derive from them asymptotic results for hitting times. For Freidlin-Wentzell Markov chains this can be done by analyzing the *energy landscape* to find the paths between the initial and the target configurations with a minimum energy barrier. In the case of the tunneling times between stable configurations of the hard-core model, this problem reduces to identifying the most efficient way, starting from a stable configuration to activate particles of the target stable configuration.

By exploring detailed geometric properties of the mixed-activity hard-core configurations on finite triangular lattices, we develop a novel combinatorial method to quantify their “energy inefficiency” and obtain in this way the *minimum energy barrier*  $\Gamma(\Lambda) > 0$  that has to be overcome in the energy landscape for the required

transition to occur. In particular, we show how this minimum energy barrier  $\Gamma(\Lambda)$  depends on the dimensions of the finite triangular lattice  $\Lambda$ .

In our main result we characterize the asymptotic behavior for the tunneling times between stable configurations giving sharp bounds in probability and proving that the order of magnitude of their expected values is equal to  $\Gamma(\Lambda)$  on a logarithmic scale. Furthermore, we prove that the tunneling times scaled by their expected values are exponentially distributed in the low-temperature limit, leveraging in a nontrivial way the intrinsic symmetry of the energy landscape.

Lastly, using structural properties of the energy landscapes and classical results [9, 34] for Friendlin-Wentzell Markov chains, we show that the timescale  $\lambda^{\Gamma(\Lambda)} = e^{\beta\Gamma(\Lambda)}$  at which transitions between maximum-occupancy configurations most likely occur is also the order of magnitude of the *mixing time* of the Markov chain  $\{X_t\}_{t \in \mathbb{N}}$ , proving that the hard-core dynamics exhibit *slow mixing* on finite triangular lattices.

## 2 Model description and main results

We consider the hard-core model on finite triangular lattices with periodic boundary conditions. More precisely, given two integers  $K \geq 2$  and  $L \geq 1$ , we consider the  $2K \times 3L$  *triangular grid*  $\Lambda$ , that is the subgraph of the triangular lattice consisting of  $N := |\Lambda| = 6KL$  sites placed on  $2K$  rows of  $3L$  sites each (or equivalently on  $6L$  columns with  $K$  sites each), see Figure 2.

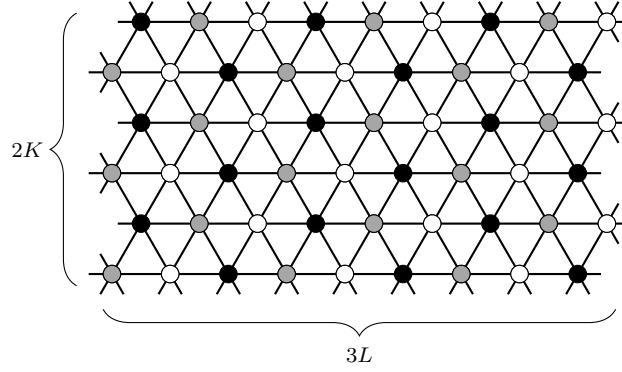


Figure 2: The  $6 \times 9$  triangular grid  $\Lambda$  and its three components highlighted using different colors

We impose periodic (wrap-around) boundary conditions on  $\Lambda$  to preserve symmetry. The triangular grid  $\Lambda$  has a natural tri-partition  $\Lambda = \Lambda_{\mathbf{a}} \cup \Lambda_{\mathbf{b}} \cup \Lambda_{\mathbf{c}}$ , which is highlighted in Figure 2 by coloring the three components in gray, black, and white, respectively. Thanks to the chosen dimensions, the three components of  $\Lambda$  have the same number of sites

$$|\Lambda_{\mathbf{a}}| = |\Lambda_{\mathbf{b}}| = |\Lambda_{\mathbf{c}}| = \frac{N}{3} = 2KL. \quad (2)$$

We associate a variable  $\sigma(v) \in \{0, 1\}$  with each site  $v \in \Lambda$ , indicating the absence (0) or the presence (1) of a particle in that site. A *hard-core configuration* is a particle configuration  $\sigma$  on  $\Lambda$  that does not violate the hard-core constraints, i.e., such that  $\sigma(v)\sigma(w) = 0$  for every pair of neighboring sites  $v, w$  of  $\Lambda$ . We denote by  $\mathcal{X} \subset \{0, 1\}^N$  the set of all hard-core configurations on  $\Lambda$ , which is in one-to-one correspondence with the collection of independent sets of the graph  $\Lambda$ .

Let  $\mathbf{a}, \mathbf{b}$  and  $\mathbf{c}$  be the hard-core configurations on the triangular grid  $\Lambda$  defined as

$$\mathbf{a}(v) := \mathbb{1}_{\{v \in \Lambda_{\mathbf{a}}\}}(v), \quad \mathbf{b}(v) := \mathbb{1}_{\{v \in \Lambda_{\mathbf{b}}\}}(v), \quad \text{and} \quad \mathbf{c}(v) := \mathbb{1}_{\{v \in \Lambda_{\mathbf{c}}\}}(v).$$

In Section 3 we show that  $\mathbf{a}, \mathbf{b}$  and  $\mathbf{c}$  are the maximum-occupancy configurations of the hard-core model on  $\Lambda$ .

We are interested in studying the Metropolis dynamics for such a model, that is the family of Markov chains  $\{X_t^\beta\}_{t \in \mathbb{N}}$  on  $\mathcal{X}$  parametrized by the inverse temperature  $\beta > 0$  with transition probabilities

$$P_\beta(\sigma, \sigma') := \begin{cases} Q(\sigma, \sigma') e^{-\beta[H(\sigma') - H(\sigma)]^+}, & \text{if } \sigma \neq \sigma', \\ 1 - \sum_{\eta \neq \sigma} P_\beta(\sigma, \eta), & \text{if } \sigma = \sigma', \end{cases}$$

where the *energy function* or *Hamiltonian*  $H : \mathcal{X} \rightarrow \mathbb{R}$  is defined as

$$H(\sigma) := - \sum_{v \in \Lambda} \sigma(v), \quad (3)$$

i.e., each configuration  $\sigma \in \mathcal{X}$  is assigned an energy  $H(\sigma)$  proportional to the total number of particles in  $\sigma$ , while the *connectivity function*  $Q : \mathcal{X} \times \mathcal{X} \rightarrow [0, 1]$  allows only single-site updates:

$$Q(\sigma, \sigma') := \begin{cases} \frac{1}{N}, & \text{if } |\{v \in \Lambda : \sigma(v) \neq \sigma'(v)\}| = 1, \\ 0, & \text{if } |\{v \in \Lambda : \sigma(v) \neq \sigma'(v)\}| > 1, \\ 1 - \sum_{\eta \neq \sigma} Q(\sigma, \eta), & \text{if } \sigma = \sigma'. \end{cases} \quad (4)$$

The triplet  $(\mathcal{X}, H, Q)$  is called *energy landscape* and we denote by  $\mathcal{X}^s$  the set of *stable configurations* of the energy landscape, that is the set of global minima of  $H$  on  $\mathcal{X}$ . Since  $\mathcal{X}$  is finite, the set  $\mathcal{X}^s$  is always nonempty.

The Markov chain  $\{X_t^\beta\}_{t \in \mathbb{N}}$  is reversible with respect to the *Gibbs measure* at inverse temperature associated to the Hamiltonian  $H$ , namely

$$\mu_\beta(\sigma) := \frac{1}{Z_\beta} e^{-\beta H(\sigma)}, \quad \sigma \in \mathcal{X},$$

where  $Z_\beta := \sum_{\sigma' \in \mathcal{X}} e^{-\beta H(\sigma')}$  is the normalizing partition function. Furthermore, it is well-known (e.g., [9, Proposition 1.1]) that the Markov chain  $\{X_t^\beta\}_{t \in \mathbb{N}}$  is aperiodic and irreducible on  $\mathcal{X}$ . Hence,  $\{X_t^\beta\}_{t \in \mathbb{N}}$  is ergodic on  $\mathcal{X}$  with stationary distribution  $\mu_\beta$ . For a nonempty subset  $A \subset \mathcal{X}$  and a configuration  $\sigma \in \mathcal{X}$ , we denote by  $\tau_A^\sigma$  the *first hitting time* of the subset  $A$  for the Markov chain  $\{X_t^\beta\}_{t \in \mathbb{N}}$  with initial configuration  $\sigma$  at time  $t = 0$ , i.e.,

$$\tau_A^\sigma := \inf\{t \in \mathbb{N} : X_t^\beta \in A \mid X_0^\beta = \sigma\}.$$

We will refer to  $\tau_A^\sigma$  as *tunneling time* if  $\sigma$  is a stable configuration and the target set is some  $A \subseteq \mathcal{X}^s \setminus \{\sigma\}$ .

The first main result describes the asymptotic behavior of the tunneling times  $\tau_{\mathbf{b}}^{\mathbf{a}}$  and  $\tau_{\{\mathbf{b}, \mathbf{c}\}}^{\mathbf{a}}$  on the triangular grid  $\Lambda$  in the low-temperature regime  $\beta \rightarrow \infty$ . More specifically, we prove the existence and find the value of an exponent  $\Gamma(\Lambda) > 0$  that appears in the asymptotic upper and lower bounds in probability for these hitting times and characterizes the asymptotic order of magnitude of their expected values as  $\beta \rightarrow \infty$ . Furthermore, we show that the tunneling times  $\tau_{\mathbf{b}}^{\mathbf{a}}$  and  $\tau_{\{\mathbf{b}, \mathbf{c}\}}^{\mathbf{a}}$  normalized by their respective means converge in distribution to an exponential unit-mean random variable.

**Theorem 2.1** (Asymptotic behavior of tunneling times). *Consider the Metropolis Markov chain  $\{X_t^\beta\}_{t \in \mathbb{N}}$  corresponding to the hard-core dynamics on the  $2K \times 3L$  triangular grid  $\Lambda$  and define*

$$\Gamma(\Lambda) := \min\{K, 2L\} + 1. \quad (5)$$

Then,

- (i)  $\lim_{\beta \rightarrow \infty} \mathbb{P}_\beta \left( e^{\beta(\Gamma(\Lambda) - \varepsilon)} \leq \tau_{\mathbf{b}}^{\mathbf{a}} \leq \tau_{\{\mathbf{b}, \mathbf{c}\}}^{\mathbf{a}} \leq e^{\beta(\Gamma(\Lambda) + \varepsilon)} \right) = 1;$
- (ii)  $\lim_{\beta \rightarrow \infty} \frac{1}{\beta} \log \mathbb{E} \tau_{\mathbf{b}}^{\mathbf{a}} = \Gamma(\Lambda) = \lim_{\beta \rightarrow \infty} \frac{1}{\beta} \log \mathbb{E} \tau_{\{\mathbf{b}, \mathbf{c}\}}^{\mathbf{a}};$
- (iii)  $\frac{\tau_{\{\mathbf{b}, \mathbf{c}\}}^{\mathbf{a}}}{\mathbb{E} \tau_{\{\mathbf{b}, \mathbf{c}\}}^{\mathbf{a}}} \xrightarrow{d} \text{Exp}(1), \quad \text{as } \beta \rightarrow \infty;$
- (iv)  $\frac{\tau_{\mathbf{b}}^{\mathbf{a}}}{\mathbb{E} \tau_{\mathbf{b}}^{\mathbf{a}}} \xrightarrow{d} \text{Exp}(1), \quad \text{as } \beta \rightarrow \infty.$

The proofs of statements (i), (ii), and (iii) of the latter theorem are presented in Section 3 and leverage the general framework for hitting time asymptotics developed in [37] in combination with the analysis of the energy landscape corresponding to the hard-core model on the triangular grid  $\Lambda$ . Although statements (iii) and (iv) look alike, their proofs slightly differ and for this reason that of statement (iv) is given later, in Section 4. Indeed, the proof of the asymptotic exponentiality of the scaled tunneling time  $\tau_{\mathbf{b}}^{\mathbf{a}} / \mathbb{E} \tau_{\mathbf{b}}^{\mathbf{a}}$  uses a stochastic representation of the tunneling time  $\tau_{\mathbf{b}}^{\mathbf{a}}$  that exploits the symmetries that the energy landscape inherits from the nontrivial automorphisms of the triangular grid.

As established by the next theorem, which is our second main result, the structural properties of the energy landscapes that will be presented in Section 3 also yield the following result for the *mixing time*. Recall that the mixing time describes the time required for the distance (measured in total variation) to stationarity to become small. More precisely, for every  $0 < \varepsilon < 1$ , we define the *mixing time*  $t_\beta^{\text{mix}}(\varepsilon)$  by

$$t_\beta^{\text{mix}}(\varepsilon) := \min\{n \geq 0 : \max_{\sigma \in \mathcal{X}} \|P_\beta^n(\sigma, \cdot) - \mu_\beta(\cdot)\|_{\text{TV}} \leq \varepsilon\},$$

where  $\|\nu - \nu'\|_{\text{TV}} := \frac{1}{2} \sum_{\sigma \in \mathcal{X}} |\nu(\sigma) - \nu'(\sigma)|$  for any two probability distributions  $\nu, \nu'$  on  $\mathcal{X}$ . Another classical notion to investigate the speed of convergence of Markov chains is the *spectral gap*, which is defined as  $\rho_\beta := 1 - \alpha_2$ , where  $1 = \alpha_1 > \alpha_2 \geq \dots \geq \alpha_{|\mathcal{X}|} \geq -1$  are the eigenvalues of the matrix  $(P_\beta(\sigma, \sigma'))_{\sigma, \sigma' \in \mathcal{X}}$ . The spectral gap can be equivalently defined using the Dirichlet form associated with the pair  $(P_\beta, \mu_\beta)$ , see [30, Lemma 13.12].

**Theorem 2.2** (Mixing time and spectral gap). *Consider the Metropolis Markov chain  $\{X_t^\beta\}_{t \in \mathbb{N}}$  corresponding to the hard-core dynamics on the  $2K \times 3L$  triangular grid  $\Lambda$  and define  $\Gamma(\Lambda)$  as in (5). Then, for any  $0 < \varepsilon < 1$ ,*

$$\lim_{\beta \rightarrow \infty} \frac{1}{\beta} \log t_\beta^{\text{mix}}(\varepsilon) = \Gamma(\Lambda).$$

Furthermore, there exist two positive constants  $0 < c_1 \leq c_2 < \infty$  independent of  $\beta$  such that the spectral gap  $\rho_\beta$  of the Markov chain  $\{X_t^\beta\}_{t \in \mathbb{N}}$  satisfies

$$c_1 e^{-\beta \Gamma(\Lambda)} \leq \rho_\beta \leq c_2 e^{-\beta \Gamma(\Lambda)} \quad \forall \beta \geq 0.$$

Therefore, the mixing time turns out to be asymptotically of the same order of magnitude as the tunneling time between stable configurations, establishing the *slow mixing* of  $\{X_t^\beta\}_{t \in \mathbb{N}}$  as  $\beta \rightarrow \infty$ .

The rest of the paper is organized as follows. The two main theorems are proved in Section 3 apart from Theorem 2.1(iv), which is proved separately in Section 4 using renewal arguments. Section 5 is entirely devoted to analysis of geometrical and combinatorial properties of the hard-core configurations on triangular grids and to the derivation of the structural properties of the energy landscape used in Sections 3 and 4.

### 3 Energy landscape analysis

This section is devoted to the analysis of the energy landscape associated with the hard-core dynamics on the  $2K \times 3L$  triangular grid  $\Lambda$ . Leveraging geometrical features of the hard-core configurations on  $\Lambda$ , we prove crucial structural properties of the energy landscape, as stated in Theorem 3.1 below. Used in combination with the model-independent results in [37], these properties will yield Theorems 2.1(i)-(iii) and 2.2, as we show in Subsection 3.1.

In the rest of this paper, we will use the some notions and notation introduced in [37]. The connectivity matrix  $Q$  given in (4) is irreducible, i.e., for any pair of configurations  $\sigma, \sigma' \in \mathcal{X}$ ,  $\sigma \neq \sigma'$ , there exists a finite sequence  $\omega$  of configurations  $\omega_1, \dots, \omega_n \in \mathcal{X}$  such that  $\omega_1 = \sigma$ ,  $\omega_n = \sigma'$  and  $Q(\omega_i, \omega_{i+1}) > 0$ , for  $i = 1, \dots, n-1$ . We will refer to such a sequence as a *path* from  $\sigma$  to  $\sigma'$  and we will denote it by  $\omega : \sigma \rightarrow \sigma'$ . Given a path  $\omega = (\omega_1, \dots, \omega_n)$ , we define its *height*  $\Phi_\omega$  as  $\Phi_\omega := \max_{i=1, \dots, n} H(\omega_i)$ . The *communication height* between a pair of configurations  $\sigma, \sigma' \in \mathcal{X}$  is defined as

$$\Phi(\sigma, \sigma') := \min_{\omega: \sigma \rightarrow \sigma'} \Phi_\omega = \min_{\omega: \sigma \rightarrow \sigma'} \max_{i=1, \dots, |\omega|} H(\omega_i),$$

and its natural extension to disjoint non-empty subsets  $A, B \subset \mathcal{X}$  is

$$\Phi(A, B) := \min_{\sigma \in A, \sigma' \in B} \Phi(\sigma, \sigma').$$

The next theorem summarizes the structural properties that we proved for the energy landscape corresponding to the hard-core dynamics on a triangular grid  $\Lambda$ . More specifically, (i) we prove that **a**, **b** and **c** are the only three stable configurations, (ii) find the value of the communication height between them, as a function of the triangular grid dimensions  $K$  and  $L$ , and (iii) show by means of two iterative algorithms that there is “*absence of deep cycles*” (see condition (6) below) in the energy landscape  $(\mathcal{X}, H, Q)$ .

**Theorem 3.1** (Structural properties of the energy landscape). *Let  $(\mathcal{X}, H, Q)$  be the energy landscape corresponding to the hard-core dynamics on the  $2K \times 3L$  triangular grid  $\Lambda$ . Then*

- (i)  $\mathcal{X}^s = \{\mathbf{a}, \mathbf{b}, \mathbf{c}\}$ ;
- (ii)  $\Phi(\mathbf{a}, \mathbf{b}) - H(\mathbf{a}) = \Phi(\mathbf{a}, \mathbf{c}) - H(\mathbf{a}) = \Phi(\mathbf{b}, \mathbf{c}) - H(\mathbf{b}) = \min\{K, 2L\} + 1$ ;
- (iii)  $\Phi(\sigma, \{\mathbf{a}, \mathbf{b}, \mathbf{c}\}) - H(\sigma) \leq \min\{K, 2L\} \quad \forall \sigma \in \mathcal{X} \setminus \{\mathbf{a}, \mathbf{b}, \mathbf{c}\}$ .

This latter theorem motivates the definition (5) of  $\Gamma(\Lambda)$  in Theorem 2.1. The full proof of Theorem 3.1 is presented in Section 5, but we briefly outline here the proof strategy.

As illustrated by the state space diagram in Figure 3 below, there is not a unique bottleneck separating the stable configurations (this was the case for complete partite graphs [51, 52]) and there are in fact exponentially many possible ways for the Markov chain  $\{X_t^\beta\}_{t \in \mathbb{N}}$  to make such transitions. This makes the task of identifying the energy barrier between stable configurations much harder.

Inspired by the ideas in [24] and by the methodology used for square grids in [37] we tackle this problem by looking at geometric features of the hard-core configurations on triangular grids. In Subsection 5.1, after some preliminary definitions, we study the combinatorial properties of hard-core configurations on horizontal and vertical *stripes* of the triangular grid  $\Lambda$ , i.e., pairs of adjacent rows (triplets of adjacent columns, respectively).



In particular, we find the maximum number of particles that a hard-core configuration can have in a horizontal stripe and characterize how particles are arranged on such stripes in Lemma 5.2. Theorem 3.1(i) is an almost immediate consequence of these combinatorial results.

Afterwards, using geometrical properties of the hard-core configurations, we prove Proposition 5.4, which gives the following lower bound for the communication height between  $\mathbf{a}$  and  $\mathbf{b}$ :

$$\Phi(\mathbf{a}, \mathbf{b}) - H(\mathbf{a}) \geq \min\{K, 2L\} + 1.$$

We then introduce two *energy reduction algorithms* in Subsection 5.2, which are used in Proposition 5.5 to construct a reference path  $\omega^* : \mathbf{a} \rightarrow \mathbf{b}$ . Such a path shows that the lower bound above is sharp, so that

$$\Phi(\mathbf{a}, \mathbf{b}) - H(\mathbf{a}) = \min\{K, 2L\} + 1,$$

concluding the proof of Theorem 3.1(ii). The energy reduction algorithm is then used again to construct a path from every configuration  $\sigma \neq \mathbf{a}, \mathbf{b}, \mathbf{c}$  to the set  $\{\mathbf{a}, \mathbf{b}, \mathbf{c}\}$  with a prescribed energy height, proving in this way Theorem 3.1(iii).

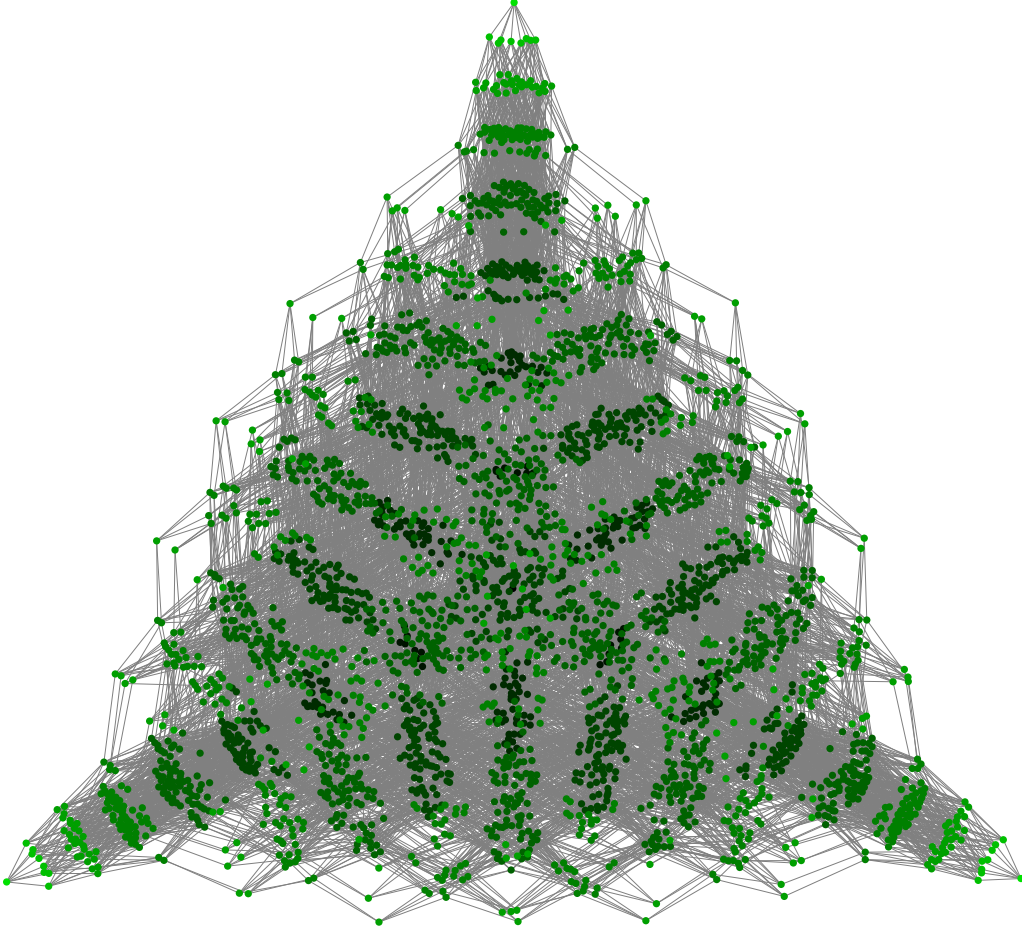


Figure 3: The energy landscape corresponding to the hard-core dynamics on the  $4 \times 6$  triangular grid. The color scheme is chosen in such a way that the lighter the color of a node, the lower the energy of the corresponding configuration.

We now briefly recall some model-independent results derived in [37] valid for any Metropolis Markov chain, that in combination with Theorem 3.1 yield the main results presented in Section 2. We present here such results only in a special case that is relevant for the tunneling times  $\tau_{\mathbf{b}}^{\mathbf{a}}$  and  $\tau_{\{\mathbf{b}, \mathbf{c}\}}^{\mathbf{a}}$  under analysis. The more general statements can be found in [37], see Corollary 3.16, Theorem 3.17 and 3.19, and Proposition 3.18 and 3.20.

**Proposition 3.2** (Hitting time asymptotics [37]). *Consider a non-empty subset  $A \subset \mathcal{X}$  and  $\sigma \in \mathcal{X} \setminus A$  and the following two conditions:*

$$\Phi(\sigma, A) - H(\sigma) = \max_{\eta \in \mathcal{X} \setminus A} \Phi(\eta, A) - H(\eta), \quad (6)$$

and

$$\Phi(\sigma, A) - H(\sigma) > \max_{\eta \in \mathcal{X} \setminus A, \eta \neq \sigma} \Phi(\eta, A \cup \{\sigma\}) - H(\eta). \quad (7)$$

(i) If (6) holds for the pair  $(\sigma, A)$ , then, setting  $\Gamma := \Phi(\sigma, A) - H(\sigma)$ , we have that for any  $\varepsilon > 0$

$$\lim_{\beta \rightarrow \infty} \mathbb{P}\left(e^{\beta(\Gamma - \varepsilon)} < \tau_A^\sigma < e^{\beta(\Gamma + \varepsilon)}\right) = 1, \quad \text{and} \quad \lim_{\beta \rightarrow \infty} \frac{1}{\beta} \log \mathbb{E} \tau_A^\sigma = \Gamma.$$

(ii) If (7) holds for the pair  $(\sigma, A)$ , then

$$\frac{\tau_A^\sigma}{\mathbb{E} \tau_A^\sigma} \xrightarrow{d} \text{Exp}(1), \quad \text{as } \beta \rightarrow \infty.$$

More precisely, there exist two functions  $k_1(\beta)$  and  $k_2(\beta)$  with  $\lim_{\beta \rightarrow \infty} k_1(\beta) = 0$  and  $\lim_{\beta \rightarrow \infty} k_2(\beta) = 0$  such that for any  $s > 0$

$$\left| \mathbb{P}\left(\frac{\tau_A^\sigma}{\mathbb{E} \tau_A^\sigma} > s\right) - e^{-s} \right| \leq k_1(\beta) e^{-(1 - k_2(\beta))s}.$$

Condition (6) says that the initial configuration  $\sigma$  has an energy barrier separating it from the target subset  $A$  that is maximum over the entire energy landscape. Informally, this means that all other “valleys” (or more formally *cycles*, see definition in [33]) of the energy landscape are not deeper than the one where the Markov chain starts; for this reason, the authors in [37] refer to (6) as “absence of deep cycles”. On the other hand, condition (7) guarantees that from any configuration  $\eta \in \mathcal{X}$  the Markov chain  $\{X_t^\beta\}_{t \in \mathbb{N}}$  reaches the set  $A \cup \{\sigma\}$  on a time scale strictly smaller than that at which the transition from  $\sigma$  to  $A$  occurs. We remark that both these conditions are sufficient, but not necessary, see [37] for further discussion.

For the proof of Theorem 2.2, we will also need the following proposition, which is also a general result concerning the asymptotic behavior of mixing time and spectral gap of any Metropolis Markov chain.

**Proposition 3.3** (Mixing time asymptotics [37, Proposition 3.24]). *For any  $0 < \varepsilon < 1$*

$$\lim_{\beta \rightarrow \infty} \frac{1}{\beta} \log t_\beta^{\text{mix}}(\varepsilon) = \lim_{\beta \rightarrow \infty} -\frac{1}{\beta} \log \rho_\beta = \Gamma^*,$$

where  $\Gamma^* := \max_{\eta \in \mathcal{X}, \eta \neq \sigma} \Phi(\eta, \sigma) - H(\eta)$  for any stable configuration  $\sigma \in \mathcal{X}^s$ . Furthermore, there exist two positive constants  $0 < c_1 \leq c_2 < \infty$  independent of  $\beta$  such that for every  $\beta \geq 0$

$$c_1 e^{-\beta \Gamma^*} \leq \rho_\beta \leq c_2 e^{-\beta \Gamma^*}.$$

### 3.1 Proofs of Theorems 2.1 and 2.2

In this subsection, we prove the two main theorems of this paper exploiting the properties of the energy landscape outlined in Theorem 3.1.

*Proof of Theorem 2.1(i)-(iii).* From Theorem 3.1(iii) it immediately follows that

$$\max_{\sigma \neq \mathbf{a}, \mathbf{b}, \mathbf{c}} \Phi(\sigma, \{\mathbf{a}, \mathbf{b}, \mathbf{c}\}) - H(\sigma) \leq \min\{K, 2L\}. \quad (8)$$

Furthermore, we claim that the following identity holds:

$$\max_{\sigma \neq \mathbf{b}, \mathbf{c}} \Phi(\sigma, \{\mathbf{b}, \mathbf{c}\}) - H(\sigma) = \min\{K, 2L\} + 1. \quad (9)$$

First notice that since  $\mathbf{a} \in \mathcal{X} \setminus \{\mathbf{b}, \mathbf{c}\}$ , we have

$$\max_{\sigma \neq \mathbf{b}, \mathbf{c}} \Phi(\sigma, \{\mathbf{b}, \mathbf{c}\}) - H(\sigma) \geq \Phi(\mathbf{a}, \{\mathbf{b}, \mathbf{c}\}) - H(\mathbf{a}) = \min\{K, 2L\} + 1.$$

In order to prove that identity (9) holds, we need to show that this lower bound is sharp. In particular, we need to show that  $\Phi(\sigma, \{\mathbf{b}, \mathbf{c}\}) - H(\sigma) \leq \min\{K, 2L\} + 1$  for every configuration  $\sigma \neq \mathbf{a}, \mathbf{b}, \mathbf{c}$ , but we will actually prove a stronger inequality, namely

$$\Phi(\sigma, \mathbf{b}) - H(\sigma) \leq \min\{K, 2L\} + 1, \quad \forall \sigma \in \mathcal{X} \setminus \{\mathbf{a}, \mathbf{b}, \mathbf{c}\}. \quad (10)$$

In Subsection 5.2 we introduce a iterative procedure that builds a path from any configuration  $\sigma$  to the set of stable configuration  $\mathcal{X}^s$ . More specifically, inspecting the proof of Theorem 3.1(iii), we notice that every configuration  $\sigma \neq \mathbf{a}, \mathbf{b}, \mathbf{c}$  can be reduced either directly to  $\mathbf{b}$ , or otherwise to  $\mathbf{a}$  or  $\mathbf{c}$ , depending on its geometrical features. If  $\sigma$  can be reduced directly to  $\mathbf{b}$ , then we prove therein that  $\Phi(\sigma, \mathbf{b}) - H(\sigma) \leq \min\{K, 2L\}$ . If not, then  $\sigma$  has to display a vertical gray or white bridge and  $K \leq 2L$ . In the proof of Theorem 3.1(iii) we construct a path  $\omega$  from  $\sigma$  to  $\mathbf{a}$  (respectively,  $\mathbf{c}$ ) such that  $\Phi_\omega \leq H(\sigma) + 2$ , which, concatenated with the reference path

from  $\mathbf{a}$  to  $\mathbf{b}$  (that will be exhibited in Proposition 5.5) or the analogous reference path from  $\mathbf{c}$  to  $\mathbf{b}$ , shows that  $\Phi(\sigma, \mathbf{b}) \leq \max\{H(\sigma) + 2, \Phi(\mathbf{a}, \mathbf{b})\}$ . Thus,

$$\begin{aligned}\Phi(\sigma, \mathbf{b}) - H(\sigma) &\leq \max\{2, \Phi(\mathbf{a}, \mathbf{b}) - H(\sigma)\} \leq \max\{2, \Phi(\mathbf{a}, \mathbf{b}) - H(\mathbf{a})\} = \max\{2, \min\{K, 2L\} + 1\} \\ &\leq \min\{K, 2L\} + 1,\end{aligned}$$

which implies that inequality (10) holds. In view of (9), the pair  $(\mathbf{a}, \{\mathbf{b}, \mathbf{c}\})$  then satisfies condition (6), since

$$\Phi(\mathbf{a}, \{\mathbf{b}, \mathbf{c}\}) - H(\mathbf{a}) = \min\{K, 2L\} + 1 = \max_{\sigma \neq \mathbf{b}, \mathbf{c}} \Phi(\sigma, \{\mathbf{b}, \mathbf{c}\}) - H(\sigma),$$

and Proposition 3.2(i) then yields statements (i) and (ii) of Theorem 2.1. Furthermore, by combining the latter identity and inequality (8), we obtain

$$\Phi(\mathbf{a}, \{\mathbf{b}, \mathbf{c}\}) - H(\mathbf{a}) = \min\{K, 2L\} + 1 > \min\{K, 2L\} \geq \max_{\sigma \neq \mathbf{a}, \mathbf{b}, \mathbf{c}} \Phi(\sigma, \{\mathbf{a}, \mathbf{b}, \mathbf{c}\}) - H(\sigma),$$

and thus condition (7) holds for the pair  $(\mathbf{a}, \{\mathbf{b}, \mathbf{c}\})$ . Proposition 3.2(ii) then yields the asymptotic exponentiality of the rescaled tunneling time  $\tau_{\{\mathbf{b}, \mathbf{c}\}}^{\mathbf{a}} / \mathbb{E}\tau_{\{\mathbf{b}, \mathbf{c}\}}^{\mathbf{a}}$ , i.e.,

$$\frac{\tau_{\{\mathbf{b}, \mathbf{c}\}}^{\mathbf{a}}}{\mathbb{E}\tau_{\{\mathbf{b}, \mathbf{c}\}}^{\mathbf{a}}} \xrightarrow{d} \text{Exp}(1), \quad \text{as } \beta \rightarrow \infty, \quad (11)$$

proving Theorem 2.1(iii).

Consider now the other tunneling time, namely  $\tau_{\mathbf{b}}^{\mathbf{a}}$ . From inequality (10) it immediately follows that

$$\max_{\sigma \neq \mathbf{b}} \Phi(\sigma, \mathbf{b}) - H(\sigma) \leq \min\{K, 2L\} + 1,$$

which, in view of Proposition 5.5, implies that

$$\Phi(\mathbf{a}, \mathbf{b}) - H(\mathbf{a}) = \min\{K, 2L\} + 1 = \max_{\sigma \neq \mathbf{b}} \Phi(\sigma, \mathbf{b}) - H(\sigma).$$

Hence the pair  $(\mathbf{a}, \{\mathbf{b}\})$  satisfies condition (6) and statements (i) and (ii) of Theorem 2.1 for the tunneling time  $\tau_{\mathbf{b}}^{\mathbf{a}}$  immediately follow from Proposition 3.2(i).  $\square$

However, the pair  $(\mathbf{a}, \{\mathbf{b}\})$  does not satisfy condition (7), due to the presence of a deep cycle (the one where configuration  $\mathbf{c}$  lies) different from the initial configuration  $\mathbf{a}$  lies. Indeed,

$$\Phi(\mathbf{a}, \mathbf{b}) - H(\mathbf{a}) \not\leq \Phi(\mathbf{c}, \mathbf{b}) - H(\mathbf{c}),$$

as shown in Theorem 3.1(ii). Hence, Theorem 2.1(iv) does not follow from the general results outlined in Proposition 3.2. The asymptotic exponentiality of the scaled hitting time  $\tau_{\mathbf{b}}^{\mathbf{a}} / \mathbb{E}\tau_{\mathbf{b}}^{\mathbf{a}}$  in the limit  $\beta \rightarrow \infty$  will be proved in the next Section 4 leveraging the symmetric structure of the energy landscape.

*Proof of Theorem 2.2.* The proof immediately follows from Proposition 3.3, since by combining inequality (10) and Theorem 3.1(ii) we get

$$\Gamma^* = \max_{\sigma \neq \mathbf{b}} \Phi(\sigma, \mathbf{b}) - H(\sigma) = \min\{K, 2L\} + 1. \quad \square$$

## 4 Asymptotic exponentiality of the tunneling time $\tau_{\mathbf{b}}^{\mathbf{a}}$

In view of the intrinsic symmetry of a triangular grid  $\Lambda$ , it is intuitive that the energy landscape  $\mathcal{X}$  on which the Markov chain  $\{X_t^\beta\}_{t \in \mathbb{N}}$  evolves is highly symmetric. In this section, we show that a  $2K \times 3L$  triangular grid has nontrivial automorphisms and discuss the consequences of this fact for the state space  $\mathcal{X}$ . We then leverage these symmetries to derive results for the tunneling time  $\tau_{\mathbf{b}}^{\mathbf{a}}$ , namely Proposition 4.1 and Corollary 4.2, and ultimately to prove Theorem 2.1(iv).

As illustrated in Section 2, the  $2K \times 3L$  triangular grid  $\Lambda$  has a natural tri-partition  $\Lambda = \Lambda_{\mathbf{a}} \cup \Lambda_{\mathbf{b}} \cup \Lambda_{\mathbf{c}}$ . Recall that the vertical and horizontal dimensions of the triangular grid  $\Lambda$  have been chosen in such a way that these three components are balanced, i.e., they comprise the same number of sites.

By considering the axial symmetries along vertical lines, we can easily construct automorphisms that swap two of these components while mapping the third one to itself. For instance, consider the axial symmetry  $\xi_{\mathbf{a}, \mathbf{b}}$  displayed in Figure 4.  $\xi_{\mathbf{a}, \mathbf{b}}$  maps  $\Lambda_{\mathbf{a}}$  (“the gray sites”) into  $\Lambda_{\mathbf{b}}$  (“the black sites”), while the sites in  $\Lambda_{\mathbf{c}}$  (“the white sites”) are only permuted.



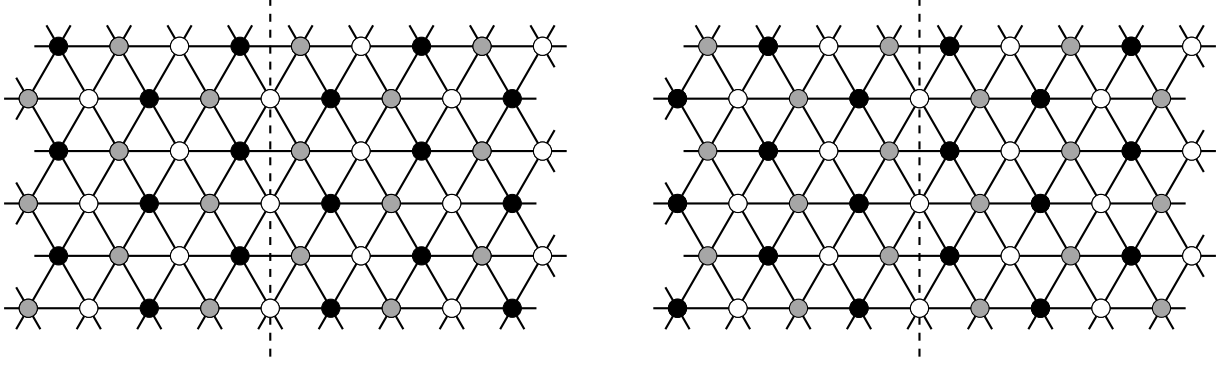


Figure 4: The automorphism  $\xi_{\mathbf{a},\mathbf{b}}$  of the  $6 \times 9$  triangular grid  $\Lambda$  induced by axial symmetry along the dashed vertical line maps gray sites into black sites (and vice-versa) while white sites are only permuted.

It is immediate that  $\xi_{\mathbf{a},\mathbf{b}}$  is indeed an automorphism of the triangular grid  $\Lambda$ , since neighboring sites are mapped into neighboring sites. Therefore,  $\xi_{\mathbf{a},\mathbf{b}}$  maps hard-core configurations into hard-core configurations and induces in this way a nontrivial permutation of the state space  $\mathcal{X}$ . Denote by  $\xi_{\mathbf{a},\mathbf{c}}$  and  $\xi_{\mathbf{b},\mathbf{c}}$  the two analogous axial symmetries of  $\Lambda$  such that

$$\xi_{\mathbf{a},\mathbf{c}}(\Lambda_{\mathbf{a}}) = \Lambda_{\mathbf{c}}, \quad \xi_{\mathbf{a},\mathbf{c}}(\Lambda_{\mathbf{c}}) = \Lambda_{\mathbf{a}}, \quad \xi_{\mathbf{a},\mathbf{c}}(\Lambda_{\mathbf{b}}) = \Lambda_{\mathbf{b}}, \quad \text{and} \quad \xi_{\mathbf{b},\mathbf{c}}(\Lambda_{\mathbf{b}}) = \Lambda_{\mathbf{c}}, \quad \xi_{\mathbf{b},\mathbf{c}}(\Lambda_{\mathbf{c}}) = \Lambda_{\mathbf{b}}, \quad \xi_{\mathbf{b},\mathbf{c}}(\Lambda_{\mathbf{a}}) = \Lambda_{\mathbf{a}}.$$

As illustrate by the next proposition, these axial symmetries of  $\Lambda$  induce automorphisms of the state space diagram  $\mathcal{X}$  corresponding to the hard-core dynamics on  $\Lambda$ . Hence, the state space  $\mathcal{X}$  is highly symmetric, as clearly visible in Figure 3, which shows the state space diagram of the hard-core model on the  $4 \times 6$  triangular grid  $\Lambda$ . Leveraging the symmetry of  $\mathcal{X}$ , we construct a coupling between different copies of the Markov chain  $\{X_t^\beta\}_{t \in \mathbb{N}}$  and prove in this way properties of the first hitting time  $\tau_{\{\mathbf{b},\mathbf{c}\}}^{\mathbf{a}}$ .

**Proposition 4.1** (Tunneling time properties). *Let  $\{X_t^\beta\}_{t \in \mathbb{N}}$  be the Metropolis Markov chain corresponding to the hard-core dynamics on a  $2K \times 3L$  triangular grid. Then, at stationarity, for every  $\beta > 0$ ,*

- (i) *The random variable  $X_{\tau_{\{\mathbf{b},\mathbf{c}\}}^{\mathbf{a}}}$  has a uniform distribution over  $\{\mathbf{b}, \mathbf{c}\}$ ;*
- (ii)  *$\tau_{\{\mathbf{b},\mathbf{c}\}}^{\mathbf{a}} \stackrel{d}{=} \tau_{\{\mathbf{a},\mathbf{c}\}}^{\mathbf{b}} \stackrel{d}{=} \tau_{\{\mathbf{a},\mathbf{b}\}}^{\mathbf{c}}$ ;*
- (iii) *The random variables  $\tau_{\{\mathbf{b},\mathbf{c}\}}^{\mathbf{a}}$  and  $X_{\tau_{\{\mathbf{b},\mathbf{c}\}}^{\mathbf{a}}}$  are independent.*

*Proof.* The automorphism  $\xi_{\mathbf{b},\mathbf{c}} : \Lambda \rightarrow \Lambda$  induces a permutation  $\bar{\xi}$  of the collection  $\mathcal{X}$  of hard-core configurations on  $\Lambda$ . More precisely,  $\bar{\xi}$  maps the hard-core configuration  $\sigma \in \mathcal{X}$  into a new configuration  $\bar{\xi}(\sigma)$  defined as

$$(\bar{\xi}(\sigma))(v) = \sigma(\xi_{\mathbf{b},\mathbf{c}}(v)) \quad \forall v \in \Lambda.$$

In fact,  $\bar{\xi}$  is an automorphism of the state space diagram, seen as a graph with vertex set  $\mathcal{X}$  and such that any pair of hard-core configurations  $\sigma, \sigma' \in \mathcal{X}$  is connected by an edge if and only if  $\sigma$  and  $\sigma'$  differ in no more than one site, i.e.,  $\|\sigma - \sigma'\| \leq 1$ . By construction,

$$\bar{\xi}(\mathbf{b}) = \mathbf{c}, \quad \bar{\xi}(\mathbf{c}) = \mathbf{b}, \quad \text{and} \quad \bar{\xi}(\mathbf{a}) = \mathbf{a}. \tag{12}$$

Assume the Metropolis Markov chain  $\{X_t^\beta\}_{t \in \mathbb{N}}$  on  $\Lambda$  starts in configuration  $\mathbf{a}$  at time 0. Let  $\{Y_t^\beta\}_{t \in \mathbb{N}}$  be the Markov chain that mimics the moves of the Markov chain  $\{X_t^\beta\}_{t \in \mathbb{N}}$  via the automorphism  $\bar{\xi}$ , i.e., set

$$Y_t^\beta := \bar{\xi}(X_t^\beta), \quad \forall t \in \mathbb{N}.$$

For notational compactness, we suppress in this proof the dependence on  $\beta$  of these two Markov chains. For any pair of hard-core configurations  $\sigma, \sigma' \in \mathcal{X}$ , any transition of the chain  $Y_t^\beta$  from  $\eta = \bar{\xi}(\sigma)$  to  $\eta' = \bar{\xi}(\sigma')$  is feasible and occurs with the same probability as the transition from  $\sigma$  to  $\sigma'$ , since  $\bar{\xi}$  is an automorphism. Therefore, the Markov chains  $\{X_t\}_{t \in \mathbb{N}}$  and  $\{Y_t\}_{t \in \mathbb{N}}$  are two copies of the hard-core dynamics on  $\Lambda$  living in the same probability space, and we have then defined in this way a coupling between them. In view of (12), this coupling immediately implies that the Markov chain  $\{X_t\}_{t \in \mathbb{N}}$  started at  $\mathbf{a}$  hits configuration  $\mathbf{b}$  precisely when the chain  $\{Y_t\}_{t \in \mathbb{N}}$  hits  $\mathbf{c}$ . Hence,

$$\mathbb{P}\left(X_{\tau_{\{\mathbf{b},\mathbf{c}\}}^{\mathbf{a}}} = \mathbf{b}, \tau_{\{\mathbf{b},\mathbf{c}\}}^{\mathbf{a}} \leq t\right) = \mathbb{P}\left(\bar{\xi}(X_{\tau_{\{\mathbf{b},\mathbf{c}\}}^{\mathbf{a}}}) = \bar{\xi}(\mathbf{b}), \tau_{\bar{\xi}(\{\mathbf{b},\mathbf{c}\})}^{\bar{\xi}(\mathbf{a})} \leq t\right) = \mathbb{P}\left(Y_{\tau_{\{\mathbf{b},\mathbf{c}\}}^{\mathbf{a}}} = \mathbf{c}, \tau_{\{\mathbf{b},\mathbf{c}\}}^{\mathbf{a}} \leq t\right). \tag{13}$$

Taking the limit  $t \rightarrow \infty$  in (13), we obtain

$$\mathbb{P}(X_{\tau_{\{\mathbf{b}, \mathbf{c}\}}^{\mathbf{a}}} = \mathbf{b}) = \mathbb{P}(Y_{\tau_{\{\mathbf{b}, \mathbf{c}\}}^{\mathbf{a}}} = \mathbf{c}).$$

Using the fact that  $\{X_t\}_{t \in \mathbb{N}}$  and  $\{Y_t\}_{t \in \mathbb{N}}$  have the same statistical law, being two copies of the same Markov chain, it then follows that the random variable  $X_{\tau_{\{\mathbf{b}, \mathbf{c}\}}^{\mathbf{a}}}$  has a uniform distribution over  $\{\mathbf{b}, \mathbf{c}\}$ , that is property (i). In particular,

$$\mathbb{P}(X_{\tau_{\{\mathbf{b}, \mathbf{c}\}}^{\mathbf{a}}} = \mathbf{b}) = \frac{1}{2}. \quad (14)$$

Let  $\hat{\xi}$  be the permutation of  $\mathcal{X}$  induced by the automorphism  $\xi_{\{\mathbf{a}, \mathbf{c}\}} \circ \xi_{\{\mathbf{a}, \mathbf{b}\}}$ . Constructing the coupling using  $\hat{\xi}$  and arguing as above, we can deduce that

$$\mathbb{P}(X_{\tau_{\{\mathbf{b}, \mathbf{c}\}}^{\mathbf{a}}} = \mathbf{b}, \tau_{\{\mathbf{b}, \mathbf{c}\}}^{\mathbf{a}} \leq t) = \mathbb{P}(\hat{\xi}(X_{\tau_{\{\mathbf{b}, \mathbf{c}\}}^{\mathbf{a}}}) = \hat{\xi}(\mathbf{b}), \tau_{\hat{\xi}(\{\mathbf{b}, \mathbf{c}\})}^{\hat{\xi}(\mathbf{a})} \leq t) = \mathbb{P}(Y_{\tau_{\{\mathbf{c}, \mathbf{a}\}}^{\mathbf{b}}} = \mathbf{c}, \tau_{\{\mathbf{c}, \mathbf{a}\}}^{\mathbf{b}} \leq t),$$

and

$$\mathbb{P}(X_{\tau_{\{\mathbf{b}, \mathbf{c}\}}^{\mathbf{a}}} = \mathbf{c}, \tau_{\{\mathbf{b}, \mathbf{c}\}}^{\mathbf{a}} \leq t) = \mathbb{P}(\hat{\xi}(X_{\tau_{\{\mathbf{b}, \mathbf{c}\}}^{\mathbf{a}}}) = \hat{\xi}(\mathbf{c}), \tau_{\hat{\xi}(\{\mathbf{b}, \mathbf{c}\})}^{\hat{\xi}(\mathbf{a})} \leq t) = \mathbb{P}(Y_{\tau_{\{\mathbf{c}, \mathbf{a}\}}^{\mathbf{b}}} = \mathbf{a}, \tau_{\{\mathbf{c}, \mathbf{a}\}}^{\mathbf{b}} \leq t).$$

Summing side by side these latter two identities yields that for every  $t \geq 0$

$$\mathbb{P}(\tau_{\{\mathbf{b}, \mathbf{c}\}}^{\mathbf{a}} \leq t) = \mathbb{P}(\tau_{\{\mathbf{c}, \mathbf{a}\}}^{\mathbf{b}} \leq t),$$

proving property (ii). Note that

$$\mathbb{P}(\tau_{\{\mathbf{b}, \mathbf{c}\}}^{\mathbf{a}} \leq t) = \mathbb{P}(X_{\tau_{\{\mathbf{b}, \mathbf{c}\}}^{\mathbf{a}}} = \mathbf{b}, \tau_{\{\mathbf{b}, \mathbf{c}\}}^{\mathbf{a}} \leq t) + \mathbb{P}(X_{\tau_{\{\mathbf{b}, \mathbf{c}\}}^{\mathbf{a}}} = \mathbf{c}, \tau_{\{\mathbf{b}, \mathbf{c}\}}^{\mathbf{a}} \leq t) = 2 \cdot \mathbb{P}(X_{\tau_{\{\mathbf{b}, \mathbf{c}\}}^{\mathbf{a}}} = \mathbf{b}, \tau_{\{\mathbf{b}, \mathbf{c}\}}^{\mathbf{a}} \leq t), \quad (15)$$

where the last passage follows from (13) using again the fact that  $\{X_t\}_{t \in \mathbb{N}}$  and  $\{Y_t\}_{t \in \mathbb{N}}$  have the same statistical law. Combining identities (14) and (15), we obtain that for every  $t \geq 0$ ,

$$\mathbb{P}(X_{\tau_{\{\mathbf{b}, \mathbf{c}\}}^{\mathbf{a}}} = \mathbf{b}, \tau_{\{\mathbf{b}, \mathbf{c}\}}^{\mathbf{a}} \leq t) = \mathbb{P}(X_{\tau_{\{\mathbf{b}, \mathbf{c}\}}^{\mathbf{a}}} = \mathbf{b}) \cdot \mathbb{P}(\tau_{\{\mathbf{b}, \mathbf{c}\}}^{\mathbf{a}} \leq t),$$

that is property (iii).  $\square$

The next corollary shows how the symmetries of the hard-core dynamics on a triangular grid  $\Lambda$  derived in Proposition 4.1 can be used to obtain a stochastic representation for the tunneling time  $\tau_{\mathbf{b}}^{\mathbf{a}}$ , that will be instrumental in the proof of Theorem 2.1(iv). The underlying idea is that, on the time-scale at which the transition from  $\mathbf{a}$  to  $\mathbf{b}$  occurs, the evolution of  $\{X_t^{\beta}\}_{t \in \mathbb{N}}$  can be represented by a 3-state Markov chain with a complete graph as state space diagram whose states correspond to the three valleys/cycles around the stable configurations  $\mathbf{a}$ ,  $\mathbf{b}$ , and  $\mathbf{c}$ . Similar ideas have been successfully used to describe metastability phenomena in [4, 28, 29].

**Corollary 4.2** (Stochastic representation of the tunneling time  $\tau_{\mathbf{b}}^{\mathbf{a}}$ ). *Let  $\{\tau^{(i)}\}_{i \in \mathbb{N}}$  be a sequence of i.i.d. random variables with common distribution  $\tau \stackrel{d}{=} \tau_{\{\mathbf{b}, \mathbf{c}\}}^{\mathbf{a}}$  and  $\mathcal{G}$  an independent geometric random variable with success probability  $1/2$ , namely  $\mathbb{P}(\mathcal{G} = m) = 2^{-m}$ , for  $m \geq 1$ . Then,*

$$\tau_{\mathbf{b}}^{\mathbf{a}} \stackrel{d}{=} \sum_{i=1}^{\mathcal{G}} \tau^{(i)}, \quad (16)$$

and, in particular,  $\mathbb{E}\tau_{\mathbf{b}}^{\mathbf{a}} = 2 \cdot \mathbb{E}\tau_{\{\mathbf{b}, \mathbf{c}\}}^{\mathbf{a}}$ . Furthermore, if additionally there exists a non-negative random variable  $Y$  such that  $\tau/\mathbb{E}\tau \xrightarrow{d} Y$  as  $\beta \rightarrow \infty$ , then

$$\frac{\tau_{\mathbf{b}}^{\mathbf{a}}}{\mathbb{E}\tau_{\mathbf{b}}^{\mathbf{a}}} \xrightarrow{d} \frac{1}{\mathbb{E}\mathcal{G}} \sum_{i=1}^{\mathcal{G}} Y^{(i)}, \quad \text{as } \beta \rightarrow \infty, \quad (17)$$

where  $\{Y^{(i)}\}_{i \in \mathbb{N}}$  is a sequence of i.i.d. random variables distributed as  $Y$ .

*Proof.* Let  $\mathcal{G}$  be the random variable counting the number of non-consecutive visits of the Markov chain to  $\{\mathbf{a}, \mathbf{c}\}$  until  $\mathbf{b}$  is hit for the first time (counting the initial configuration  $\mathbf{a}$  as first visit). In view of Proposition 4.1(i), the random variable  $\mathcal{G}$  is geometrically distributed with success probability  $\frac{1}{2}$ , with distribution  $\mathbb{P}(\mathcal{G} = m) = 2^{-m}$ , for  $m \geq 1$ . In particular,  $\mathcal{G}$  it does not depend on the inverse temperature  $\beta$ . The amount of time it takes for

the Markov chain started in a stable configuration to hit any of the other two stable configurations does not depend on the initial stable configuration, by virtue of Proposition 4.1(ii). In view of these considerations and using the independence property in Proposition 4.1(iii), we deduce the stochastic representation (16) for the tunneling time  $\tau_{\mathbf{b}}^{\mathbf{a}}$ . The identity  $\mathbb{E}\tau_{\mathbf{b}}^{\mathbf{a}} = 2 \cdot \mathbb{E}\tau_{\{\mathbf{b}, \mathbf{c}\}}^{\mathbf{a}}$  then immediately follows from Wald's identity, since both  $\mathcal{G}$  and  $\tau_{\{\mathbf{b}, \mathbf{c}\}}^{\mathbf{a}}$  have finite expectation and  $\mathbb{E}\mathcal{G} = 2$ .

Lastly, we turn to the proof of the limit in distribution (17). Denoting by  $\mathcal{L}_A(s) = \mathbb{E}(e^{-sA})$ , with  $s \geq 0$ , the Laplace transform of a random variable  $A$ , the stochastic representation (16) yields  $\mathcal{L}_{\tau_{\mathbf{b}}^{\mathbf{a}}}(s) = G_{\mathcal{G}}(\mathcal{L}_{\tau}(s))$ , where  $G_{\mathcal{G}}(\cdot)$  is the probability generating function of the random variable  $\mathcal{G}$ , i.e.,  $G_{\mathcal{G}}(z) = \mathbb{E}(z^{\mathcal{G}})$  for every  $z \in [0, 1]$ . By assumption  $\mathcal{L}_{\tau/\mathbb{E}\tau}(s) \rightarrow \mathcal{L}_Y(s)$  as  $\beta \rightarrow \infty$ . Using the fact that  $\mathbb{E}\tau_{\mathbf{b}}^{\mathbf{a}} = \mathbb{E}\tau \cdot \mathbb{E}\mathcal{G}$  we obtain

$$\mathcal{L}_{\tau_{\mathbf{b}}^{\mathbf{a}}/\mathbb{E}\tau_{\mathbf{b}}^{\mathbf{a}}}(s) = G_{\mathcal{G}}(\mathcal{L}_{\tau/\mathbb{E}\tau}(s/\mathbb{E}\mathcal{G})) \xrightarrow{\beta \rightarrow \infty} G_{\mathcal{G}}(\mathcal{L}_Y(s/\mathbb{E}\mathcal{G})),$$

and the continuity theorem for Laplace transforms yields the conclusion.  $\square$

*Proof of Theorem 2.1(iv).* Corollary 4.2 yields

$$\frac{\tau_{\mathbf{b}}^{\mathbf{a}}}{\mathbb{E}\tau_{\mathbf{b}}^{\mathbf{a}}} \xrightarrow{d} \frac{1}{2} \sum_{i=1}^{\text{Geo}(1/2)} Y^{(i)}, \quad \text{as } \beta \rightarrow \infty,$$

where  $\{Y^{(i)}\}_{i \in \mathbb{N}}$  are i.i.d. exponential random variables, in view of (11). The statement in Theorem 2.1(iv) then follows by noticing that a geometric sum of i.i.d. exponential random variables scaled by its mean is also exponentially distributed with unit mean.  $\square$

## 5 Proofs

This section is entirely devoted to the proof of the structural properties of the energy landscape summarized in Theorem 3.1. In Subsection 5.1 we first introduce some useful definitions and prove some geometrical and combinatorial properties of hard-core configurations. These will then be leveraged to prove a lower bound for the communication height between stable configurations, see Proposition 5.4, and Theorem 3.1(i). Later, in Subsection 5.2 we introduce two iterative procedures called *energy reduction algorithms* to construct paths in the energy landscape  $\mathcal{X}$  with prescribed energy height and use them to prove Theorem 3.1(ii)-(iii). In the rest of this section, we will tacitly assume that  $\Lambda$  is a  $2K \times 3L$  triangular grid with  $K \geq 2$  and  $L \geq 1$ .

### 5.1 Geometrical properties of hard-core configurations

We first introduce some useful definitions to describe hard-core configurations on the triangular grid  $\Lambda$ . Denote by  $c_j$ ,  $j = 0, \dots, 6L - 1$ , the  $j$ -th column of  $\Lambda$ , and by  $r_i$ ,  $i = 0, \dots, 2K - 1$ , the  $i$ -th row of  $\Lambda$ , see Figure 5.

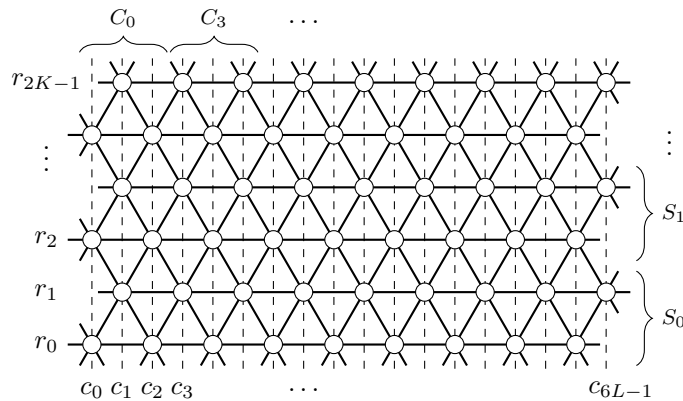


Figure 5: Illustration of row, column and stripe notation for the triangular grid

Note that every row has an equal number of sites from each component, since

$$|r_i \cap \Lambda_{\mathbf{a}}| = |r_i \cap \Lambda_{\mathbf{b}}| = |r_i \cap \Lambda_{\mathbf{c}}| = L \quad \forall i = 0, \dots, 2K - 1, \quad (18)$$

while each column consists of sites from a single component, and, in fact,

$$\Lambda_{\mathbf{a}} = \bigcup_{j=0}^{L-1} c_{3j}, \quad \Lambda_{\mathbf{b}} = \bigcup_{j=0}^{L-1} c_{3j+1}, \quad \text{and} \quad \Lambda_{\mathbf{c}} = \bigcup_{j=0}^{L-1} c_{3j+2}. \quad (19)$$

Each site  $v \in \Lambda$  lies at the intersection of a row with a column and we associate to  $v$  the coordinates  $(i, j)$  if  $v = r_i \cap c_j$ . We call the collection of sites belonging to two adjacent rows a *horizontal stripe*. In particular, we denote by  $S_i$ , with  $i = 0, \dots, K-1$ , the horizontal stripe consisting of rows  $r_{2i}$  and  $r_{2i+1}$ , i.e.,  $S_i := r_{2i} \cup r_{2i+1}$ , see Figure 5. When the index of a stripe is not relevant, we will simply denote it by  $S$ . We define a *vertical stripe* to be the collection of sites belonging to three adjacent columns, which we denote by  $C$  in general. In particular, for  $j = 0, \dots, 3L-1$  we denote by  $C_j$  the vertical stripe consisting of columns  $c_j, c_{j+1}$  and  $c_{j+2}$  (note that the indices should be taken modulo  $3L$ ), see Figure 5. For every horizontal stripe  $S$  note that  $|S| = 6L$  and (18) implies that  $|S \cap \Lambda_{\mathbf{a}}| = |S \cap \Lambda_{\mathbf{b}}| = |S \cap \Lambda_{\mathbf{c}}| = 2L$ , see also Figure 6a where we highlight the tripartition of a horizontal stripe. Similarly, for every vertical stripe  $C$ , we have  $|C| = 3K$  and, in view of (19), we have  $|C \cap \Lambda_{\mathbf{a}}| = |C \cap \Lambda_{\mathbf{b}}| = |C \cap \Lambda_{\mathbf{c}}| = K$ . A special role will be played by the vertical stripes whose middle column belongs to  $\Lambda_{\mathbf{b}}$ , which are those of the form  $C_{3j}$  for some  $j = 0, \dots, 2L-1$ , whose structure is displayed in Figures 6b and 6c.

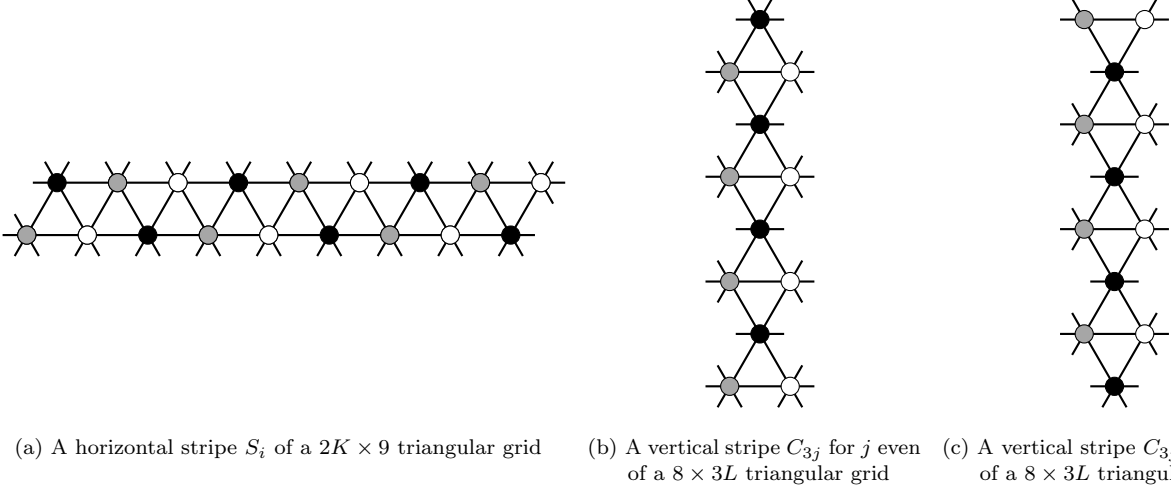


Figure 6: Illustration of horizontal and vertical stripes in which the sites' tripartition is highlighted using different colors

Given a hard-core configuration  $\sigma \in \mathcal{X}$ , we define its *energy difference*  $\Delta H(\sigma)$  as

$$\Delta H(\sigma) := H(\sigma) - H(\mathbf{a}). \quad (20)$$

In view of the fact that  $H(\mathbf{a}) = H(\mathbf{b}) = H(\mathbf{c}) = -2KL$  and the definition (3) of  $H(\cdot)$ , we can rewrite

$$\Delta H(\sigma) = 2KL - \sum_{v \in \Lambda} \sigma(v).$$

Furthermore, we define the energy difference of a configuration  $\sigma \in \mathcal{X}$  on the horizontal stripe  $S$  by

$$\Delta H_S(\sigma) := 2L - \sum_{v \in S} \sigma(v), \quad (21)$$

and the energy difference of a configuration  $\sigma \in \mathcal{X}$  on the vertical stripe  $C$  by

$$\Delta H_C(\sigma) := K - \sum_{v \in C} \sigma(v).$$

Note that the energy difference  $\Delta H(\sigma)$  in (20) can be written as the sum of the energy differences on horizontal stripes (or on non-overlapping vertical stripes), i.e.,

$$\Delta H(\sigma) = \sum_{i=0}^{K-1} \Delta H_{S_i}(\sigma) = \sum_{j=0}^{2L-1} \Delta H_{C_{3j}}(\sigma) = \sum_{j=0}^{2L-1} \Delta H_{C_{3j+1}}(\sigma) = \sum_{j=0}^{2L-1} \Delta H_{C_{3j+2}}(\sigma). \quad (22)$$

In the rest of the paper, we adopt the following coloring conventions for displaying a hard-core configuration  $\sigma \in \mathcal{X}$ : We put a node in site  $v \in \Lambda$  if it is occupied, i.e.,  $\sigma(v) = 1$ , and we color it gray, black, or white depending on whether the site  $v$  belongs to  $\Lambda_{\mathbf{a}}$ ,  $\Lambda_{\mathbf{b}}$ ,  $\Lambda_{\mathbf{c}}$  respectively; if instead a site  $v \in \Lambda$  is vacant, i.e.,  $\sigma(v) = 0$ , we do not display any node there. Figure 7a displays a hard-core configuration using this color convention.

There is an equivalent way to represent hard-core configurations. First notice that each *triangle* (e.g., each triangular face of the graph  $\Lambda$ ) can have at most one occupied particle in its three vertices, being a clique. We

adopt the following coloring convention for triangles: If a triangle has a particle in one of its three vertices, we color it gray, black or with a dashed pattern, depending on whether such particle belongs to  $\Lambda_{\mathbf{a}}$ ,  $\Lambda_{\mathbf{b}}$  or  $\Lambda_{\mathbf{c}}$ , respectively. Instead, we leave a triangle blank if none of its three vertices is occupied by a particle. Figure 7b displays the coloring corresponding to the hard-core configuration of Figure 7a. Hence, placing particles with hard-core constraints on a triangular grid corresponds to placing hexagons on the same lattice without overlaps. This is the reason why the hard-core model on the triangular lattice is often called *hard-hexagon model* in the statistical physics literature. Note that our coloring scheme implies that hexagons of different colors cannot share an edge.

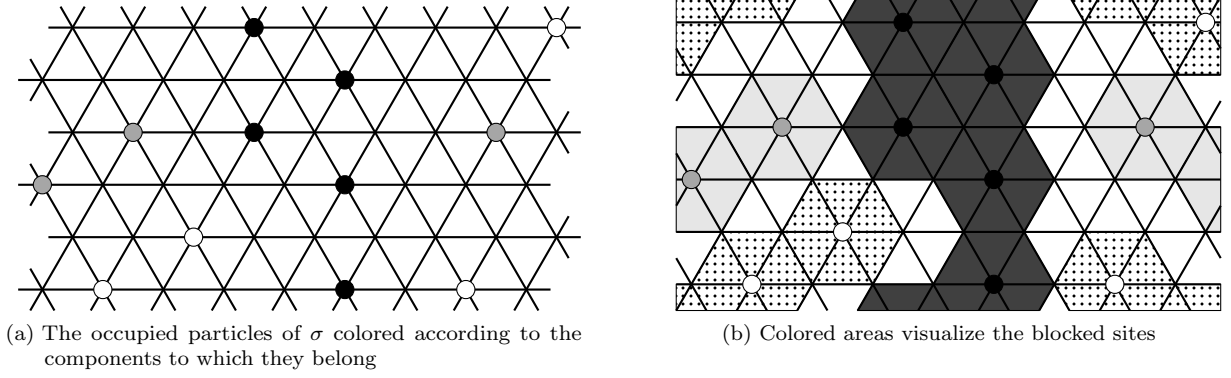


Figure 7: An example of a hard-core configuration  $\sigma$  on the  $6 \times 9$  triangular grid

Given two configurations  $\sigma, \sigma' \in \mathcal{X}$  and a subset of sites  $W \subseteq \Lambda$ , we write

$$\sigma|_W = \sigma'|_W \iff \sigma(v) = \sigma'(v) \quad \forall v \in W.$$

We say that a configuration  $\sigma \in \mathcal{X}$  has a *gray (black, white) horizontal bridge* in stripe  $S$  if  $\sigma$  perfectly agrees there with  $\mathbf{a}$  (respectively  $\mathbf{b}$ ,  $\mathbf{c}$ ), i.e.,  $\sigma|_S = \mathbf{a}|_S$  (respectively  $\sigma|_S = \mathbf{b}|_S$  or  $\sigma|_S = \mathbf{c}|_S$ ). Similarly, we say that a configuration  $\sigma \in \mathcal{X}$  has a *gray (black, white) vertical bridge* in stripe  $C$  if  $\sigma$  perfectly agrees there with  $\mathbf{a}$  (respectively  $\mathbf{b}$ ,  $\mathbf{c}$ ), i.e.,  $\sigma|_C = \mathbf{a}|_C$  (respectively  $\sigma|_C = \mathbf{b}|_C$  or  $\sigma|_C = \mathbf{c}|_C$ ). Two examples of bridges are shown in Figures 8a and 8b.

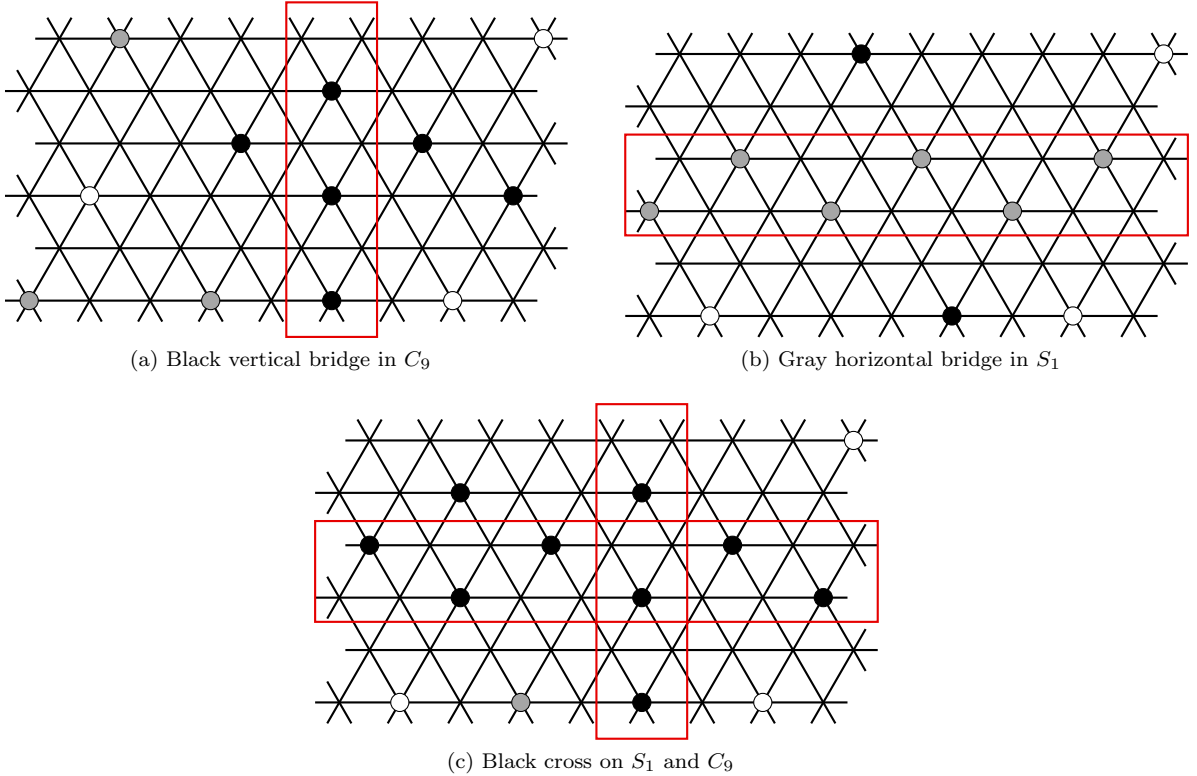


Figure 8: Examples of hard-core configurations displaying bridges or crosses on the  $6 \times 9$  triangular grid



**Lemma 5.1** (Geometric features of hard-core configurations). *A hard-core configuration  $\sigma \in \mathcal{X}$  cannot display simultaneously a vertical bridge and a horizontal bridge of different colors.*

*Proof.* We may assume that the vertical bridge is black, without loss of generality. Such a vertical bridge blocks two sites on every row, one belonging to  $\Lambda_{\mathbf{a}}$  and one to  $\Lambda_{\mathbf{c}}$  and thus no horizontal stripe can fully agree with  $\mathbf{a}$  or  $\mathbf{c}$ .  $\square$

It is possible, however, that a vertical and a horizontal bridge coexist when they are of the same color and this fact motivates the next definition. We say that a configuration  $\sigma \in \mathcal{X}$  has a *gray (black, white) cross* if it has simultaneously at least two gray (black, white) bridges, one vertical and one horizontal; see Figure 8c for an example of a black cross.

**Lemma 5.2** (Efficient horizontal stripes structure). *Consider a hard-core configuration  $\sigma \in \mathcal{X}$  on the  $2K \times 3L$  triangular grid. For every horizontal stripe  $S$ , the energy difference is non-negative, i.e.,  $\Delta H_S(\sigma) \geq 0$ , and*

$$\Delta H_S(\sigma) = 0 \iff \sigma \text{ has a horizontal bridge in stripe } S. \quad (23)$$

*Proof.* We first prove that the energy difference  $\Delta H_S(\sigma) \geq 0$  and later prove (23).

Suppose by contradiction that there exists a hard-core configuration  $\sigma$  and a horizontal stripe  $S = r \cup r'$  such that  $\Delta H_S(\sigma) < 0$ . Let  $p$  and  $p'$  the number of particles that  $\sigma$  has in rows  $r$  and  $r'$ , respectively. By definition (21), this implies that  $\sigma$  has at least  $2L + 1$  particles in stripe  $S$ , which means that one of the two rows of  $S$ , say  $r$ , must have at least  $L + 1$  particles, i.e.,  $p \geq L + 1$ . Due to the structure of a horizontal stripe, each particle on  $r$  blocks two sites in row  $r'$  and no site in row  $r'$  is blocked simultaneously by two particles in row  $r$ , since to do so such particles should reside in adjacent sites. Hence, there are at least  $2p$  blocked sites, so that in row  $r'$  there can be at most  $3L - 2p$  particles. In view of the assumption  $p \geq L + 1$ , this means that there are at most  $p + (3L - 2p) = 3L - p \leq 2L - 1$  particles in stripe  $S$ , and thus  $\Delta H_S(\sigma) > 0$ , which is a contradiction.

Let us turn to the characterization (23) of the stripes with energy difference equal to zero. If  $\sigma$  displays a bridge in a horizontal stripe  $S$ , then by definition  $\sigma|_S = \mathbf{a}|_S$  or  $\sigma|_S = \mathbf{b}|_S$  or  $\sigma|_S = \mathbf{c}|_S$ . In all three cases, we have  $\sum_{v \in S} \sigma(v) = 2L$  and thus  $\Delta H_S(\sigma) = 2L - \sum_{v \in S} \sigma(v) = 0$ .

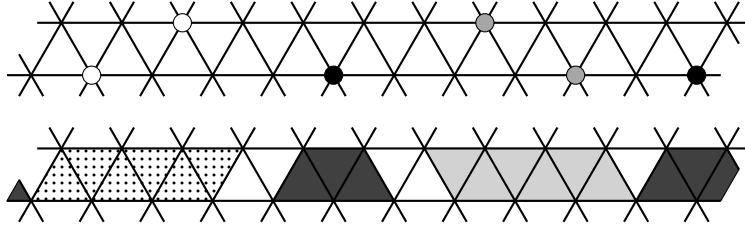


Figure 9: Equivalent representation of a hard-core configuration in a horizontal stripe of a  $2K \times 12$  triangular grid

For the converse implication, we leverage the equivalent representation of a hard-core configuration as hard hexagon introduced earlier in this section. Note that in a horizontal stripe, we see only half of any hexagon: This means that any particle blocks exactly 3 triangles on that stripe. We distinguish between blocked and free triangles and color the blocked triangles according to which particle blocks them. Denote by  $b(S)$  the number of blocked triangles in stripe  $S$  and by  $f(S)$  the number of free triangles on the same stripe. Since the total number of triangles of stripe  $S$  is  $6L$ , we have  $b(S) + f(S) = 6L$ . Furthermore, as argued before, every particle blocks exactly 3 triangles on that stripe, i.e.,  $b(S) = 3 \sum_{v \in S} \sigma(v)$ . Therefore,

$$f(S) = 6L - b(S) = 3 \left( 2L - \sum_{v \in S} \sigma(v) \right) = 3 \cdot \Delta H_S(\sigma). \quad (24)$$

Suppose now by contradiction that  $\sigma$  does not have a horizontal bridge in stripe  $S$ . If  $\sigma$  has only particles of the same color on  $S$ , then the number of particles must be strictly less than  $2L$  and thus  $\Delta H_S(\sigma) > 0$ . If instead  $\sigma$  has at least a pair of particles belonging to different components, then there exist blocked triangles of different colors. The hard-hexagon representation implies that two blocked triangles of different color cannot be adjacent, so there must be at least one free triangle separating them, i.e.,  $f(S) > 0$ , which implies that  $\Delta H_S(\sigma) > 0$  in view of (24).  $\square$

*Proof of Theorem 3.1(i).* Lemma 5.2 guarantees that  $\Delta H_S(\sigma) \geq 0$  on every horizontal stripe  $S$ . By definition (21), this means that on every horizontal stripe there can be at most  $2L$  particles. Hence

$$\max_{\sigma \in \mathcal{X}} \sum_{v \in \Lambda} \sigma(v) \leq 2KL.$$

Configurations **a**, **b** and **c** have precisely  $2KL$  particles each, in view of (2). Suppose by contradiction that there exists another configuration  $\sigma \in \mathcal{X} \setminus \{\mathbf{a}, \mathbf{b}, \mathbf{c}\}$  that has  $2KL$  particles. By definitions (20) and (21) such a configuration should be such that  $\Delta H_{S_i}(\sigma) = 0$  on every horizontal stripe  $S_i$ ,  $i = 0, \dots, K-1$ . By Lemma 5.2 configuration  $\sigma$  then has a horizontal bridge in each of these  $K$  stripes. Since two horizontal bridges of different colors cannot reside in adjacent stripes, it follows that all  $K$  bridges should be monochromatic and thus  $\sigma \in \{\mathbf{a}, \mathbf{b}, \mathbf{c}\}$ , which is a contradiction.  $\square$

In order to prove Theorem 3.1(ii), we need the following lemma for vertical stripes, which is a complementary result of Lemma 5.2 characterizing the structure of vertical stripes with zero energy difference.

**Lemma 5.3** (Efficient vertical stripes structure). *Consider a hard-core configuration  $\sigma \in \mathcal{X}$  on the  $2K \times 3L$  triangular grid. For every vertical stripe  $C$  of the form  $C = C_{3j}$ , the energy difference is non-negative, i.e.,  $\Delta H_C(\sigma) \geq 0$ . Furthermore, if  $\sigma$  has at least one black particle on  $C$ , then*

$$\Delta H_C(\sigma) = 0 \iff \sigma \text{ has a black vertical bridge in stripe } C. \quad (25)$$

*Proof.* Consider a vertical stripe  $C$  of the form  $C_{3j}$ , whose middle column is a subset of  $\Lambda_{\mathbf{b}}$ . We first prove that the energy difference  $\Delta H_C(\sigma) \geq 0$  and later prove (25). Observe that, due to the structure of the vertical stripe  $C$ , a hard-core configuration cannot have more than one particle in every row in  $C$  and, moreover, it cannot have particles residing in adjacent rows in  $C$ . From these two observations, it follows that there are no hard-core configurations with  $K+1$  or more particles on the vertical stripe  $C$  and thus  $\Delta H_C(\sigma) \geq 0$ .

If  $\sigma$  displays a vertical black bridge in vertical stripe  $C$ , then by definition  $\sigma|_C = \mathbf{b}|_C$  and thus trivially  $\Delta H_C(\sigma) = 2L - \sum_{v \in C} \sigma(v) = 0$ .

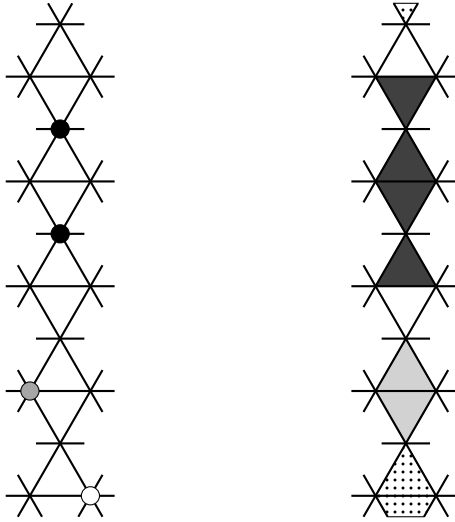


Figure 10: Equivalent representation of a hard-core configuration in a vertical stripe of a  $10 \times 3L$  triangular grid

Similarly to what we have done in the proof of Lemma 5.2, we prove the converse implication using again the equivalent representation of a hard-core configuration as hard hexagons. Note that in a vertical stripe, we see only part of these hexagons; in particular, any particle blocks exactly 2 triangles on that stripe, as illustrated in Figure 10. We distinguish between blocked and free triangles and color the blocked triangles according to which particle blocks them. A key observation is that in such a vertical stripe, dashed and gray triangles can be adjacent to each other, as shown in Figure 10, but a black triangle cannot be adjacent to a triangle of different color. Denote by  $b(C)$  the number of blocked triangles in stripe  $C$  and by  $f(C)$  the number of free triangles on the same stripe. Since the total number of triangles in stripe  $C$  is  $2K$ , we have  $b(C) + f(C) = 2K$ . Furthermore, since every particle blocks exactly 2 triangles on that vertical stripe, we have  $b(C) = 2 \sum_{v \in C} \sigma(v)$ . Therefore,

$$f(C) = 2K - b(C) = 2 \left( K - \sum_{v \in C} \sigma(v) \right) = 2 \cdot \Delta H_C(\sigma). \quad (26)$$

Suppose by contradiction that  $\sigma$  does not have a vertical black bridge in stripe  $C$ . If  $\sigma$  has only black particles on  $C$ , then the number of black particles must be strictly less than  $2K$  and thus  $\Delta H_C(\sigma) > 0$ . Instead, if  $\sigma$  has also at least one non-black particle in stripe  $C$ , then such particle blocks two triangles, which will then be non-black. Such triangles cannot be adjacent to the two black ones which exist by assumption, so there exists at least one free triangle separating them, i.e.,  $f(C) > 0$ , which implies that  $\Delta H_C(\sigma) > 0$  in view of (26).  $\square$

We are now ready to state and prove the lower bound on the communication height between any pair of stable configurations.

**Proposition 5.4** (Lower bound on the communication height between  $\mathbf{a}$  and  $\mathbf{b}$ ). *The communication height between  $\mathbf{a}$  and  $\mathbf{b}$  in the energy landscape corresponding to the hard-core model on the  $2K \times 3L$  triangular grid satisfies the following inequality*

$$\Phi(\mathbf{a}, \mathbf{b}) - H(\mathbf{a}) \geq \min\{K, 2L\} + 1.$$

*Proof.* We will show that in every path  $\omega : \mathbf{a} \rightarrow \mathbf{b}$  there exists at least one configuration with energy difference greater than or equal to  $\min\{K, 2L\} + 1$ . Consider a path  $\omega = (\omega_1, \dots, \omega_n)$  from  $\mathbf{a}$  to  $\mathbf{b}$ . Without loss of generality, we may assume that there are no void moves in  $\omega$ , i.e., at every step either a particle is added or a particle is removed, so that  $H(\omega_{i+1}) = H(\omega_i) \pm 1$  for every  $1 \leq i \leq n-1$ . Since configuration  $\mathbf{a}$  has no black bridges, while  $\mathbf{b}$  does, at some point along the path  $\omega$  there must be a configuration which is the first to display a black bridge, that is a column or a row occupied only by black particles. Denote by  $m^*$  the index corresponding to such configuration, i.e.,

$$m^* := \{m \leq n \mid \exists i : (\omega_m)_{|r_i} = \mathbf{b}_{|r_i} \text{ or } \exists j : (\omega_m)_{|c_j} = \mathbf{b}_{|c_j}\}.$$

Since a black bridge cannot be created in only two steps starting from  $\mathbf{a}$ , we must have  $m^* > 2$ . We claim that

$$\max\{\Delta H(\omega_{m^*-1}), \Delta H(\omega_{m^*-2})\} \geq \min\{K, 2L\} + 1.$$

Since the addition of a single black particle cannot create more than one bridge in each direction, it is enough to consider the following three cases:

- (a)  $\omega_{m^*}$  displays a black vertical bridge only;
- (b)  $\omega_{m^*}$  displays a black horizontal bridge only;
- (c)  $\omega_{m^*}$  displays a black cross.

For case (a), note that configuration  $\omega_{m^*}$  does not have any horizontal bridge. Indeed, it cannot have a black horizontal bridge, otherwise we would be in case (c), and any gray or white horizontal bridge cannot coexist with the black vertical bridge, in view of Lemma 5.1. Hence, the energy difference of every horizontal stripe is strictly positive, thanks to Lemma 5.2 and thus

$$\Delta H(\omega_{m^*}) = \sum_{i=0}^{K-1} \Delta H_{S_i}(\omega_{m^*}) \geq K.$$

Furthermore, configurations  $\omega_{m^*-1}$  and  $\omega_{m^*}$  differ in a unique site  $v^* \in \Lambda_{\mathbf{b}}$ , which is such that  $\omega_{m^*-1}(v^*) = 0$  and  $\omega_{m^*}(v^*) = 1$ . Hence,  $\Delta H(\omega_{m^*-1}) = \Delta H(\omega_{m^*}) + 1$  and thus

$$\Delta H(\omega_{m^*-1}) \geq K + 1.$$

The argument for case (b) is similar to that of case (a). Firstly, configuration  $\omega_{m^*}$  does not display any vertical bridge. Lemma 5.1 implies that there cannot be any gray or white vertical bridge due to the presence of a black horizontal bridge and a black vertical bridge cannot exist, otherwise there would be a black cross and we would be in case (c). Every vertical stripe has at least one black particle, due to the presence of a black horizontal bridge. Hence,  $\Delta H_{C_j}(\omega_{m^*}) \geq 1$  for every  $j = 0, \dots, 2L-1$  in view of Lemma 5.3. Therefore,

$$\Delta H(\omega_{m^*}) = \sum_{j=0}^{2L-1} \Delta H_{C_j}(\omega_{m^*}) \geq 2L.$$

From this inequality it follows that  $\Delta H(\omega_{m^*-1}) \geq 2L + 1$ , because, as for case (a), the definition of  $m^*$  implies  $\Delta H(\omega_{m^*-1}) = \Delta H(\omega_{m^*}) + 1$ .

Consider now case (c), in which  $\omega_{m^*}$  displays a black cross. The presence of both a vertical and a horizontal black bridge means that  $\omega_{m^*}$  has a black particle in every vertical and horizontal stripe. This property is inherited by the configuration  $\omega_{m^*-1}$ , since it differs from  $\omega_{m^*}$  only by the removal of the black particle lying at the intersection of the vertical and horizontal bridge constituting the cross. Furthermore, by definition of  $m^*$ , configuration  $\omega_{m^*-1}$  cannot have any black bridge, neither vertical nor horizontal. These two facts, in combination with Lemmas 5.2 and 5.3, imply that

$$\Delta H(\omega_{m^*-1}) \geq \min\{K, 2L\}.$$

If  $\Delta H(\omega_{m^*-1}) \geq \min\{K, 2L\} + 1$ , then the proof is completed. Otherwise, the energy difference of configuration  $\omega_{m^*-1}$  is  $\Delta H(\omega_{m^*-1}) = \min\{K, 2L\}$ . The configuration preceding  $\omega_{m^*-1}$  in the path  $\omega$  satisfies

$$\Delta H(\omega_{m^*-2}) = \min\{K, 2L\} \pm 1, \quad (27)$$

since it differs from  $\omega_{m^*-1}$  by a single site update. Suppose first that

$$\Delta H(\omega_{m^*-2}) = \min\{K, 2L\} - 1. \quad (28)$$

This means that  $\omega_{m^*-2}$  differs from  $\omega_{m^*-1}$  by the addition of a particle. Therefore, also configuration  $\omega_{m^*-2}$  has at least one black particle in every horizontal stripe, i.e.,

$$\sum_{v \in S_i \cap \Lambda_{\mathbf{b}}} \omega_{m^*-2}(v) \geq 1 \quad \forall i = 0, \dots, K, \quad (29)$$

and at least one black particle in every vertical stripe, i.e.,

$$\sum_{v \in C_j \cap \Lambda_{\mathbf{b}}} \omega_{m^*-2}(v) \geq 1 \quad \forall j = 0, \dots, 2L - 1. \quad (30)$$

If  $K \leq 2L$ , (28) and the pigeonhole principle imply that there must be a horizontal stripe  $S$  such that  $\Delta H_S(\omega_{m^*-2}) = 0$ . In view of (29) and Lemma 5.2,  $\omega_{m^*-2}$  must have a horizontal black bridge in  $S$ , which contradicts the definition of  $m^*$ . When instead  $K > 2L$ , it follows from (28) that there must be a vertical stripe  $C$  such that  $\Delta H_C(\omega_{m^*-2}) = 0$ . Also in this case, (30) and Lemma 5.3 imply that  $\omega_{m^*-2}$  displays a vertical black bridge in  $C$ , in contradiction with the definition of  $m^*$ . We have in this way proved that assumption (28) always leads to a contradiction, so in view of (27) we have  $\Delta H(\omega_{m^*-2}) = \min\{K, 2L\} + 1$  and the proof is concluded also for case (c).  $\square$

## 5.2 Reference path and absence of deep cycles

In this subsection we describe two iterative procedures that construct a path from a suitable initial configuration  $\sigma$  to a target stable configuration. The first one modifies the original configuration row by row and we will refer to it as *energy reduction algorithm by rows*. The second one proceeds instead by modifying  $\sigma$  column by column and, for this reason, we will call it *energy reduction algorithm by columns*. These two procedures are similar in spirit, but need to be described separately, since for the triangular grid the structure of horizontal and vertical stripes is fundamentally different. Such energy reduction algorithms will be used in Proposition 5.5 to construct the reference path from  $\mathbf{a}$  to  $\mathbf{b}$  and in the proof of Theorem 3.1(iii).

### Energy reduction algorithm by rows

We now describe in detail the energy reduction algorithm by rows with  $\mathbf{b}$  as target configuration. In order for  $\sigma \in \mathcal{X}$  to be a suitable initial configuration for this iterative procedure, we require that  $\sigma$  has no gray or white particles in the first horizontal stripe  $S_0 = r_0 \cup r_1$ , i.e.,

$$\sigma(v) = 0 \quad \forall v \in S_0 \cap (\Lambda_{\mathbf{a}} \cup \Lambda_{\mathbf{c}}). \quad (31)$$

Figure 11 shows a hard-core configuration that satisfies this initial condition.

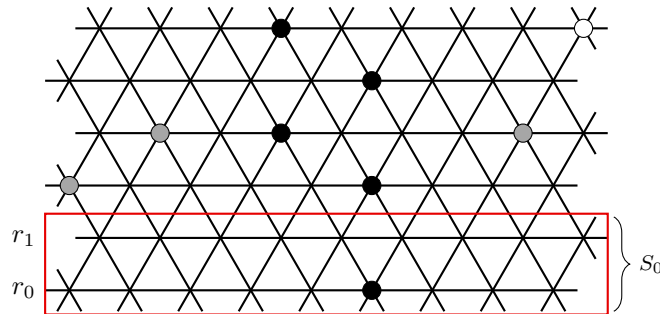


Figure 11: Example of a hard-core configuration on the  $6 \times 9$  triangular grid that satisfies (31)

The path  $\omega$  is the concatenation of  $2K$  paths  $\omega^{(1)}, \dots, \omega^{(2K)}$ . For every  $i = 1, \dots, 2K$ , path  $\omega^{(i)}$  goes from  $\sigma_i$  to  $\sigma_{i+1}$ , where we set  $\sigma_1 := \sigma$ ,  $\sigma_{2K+1} := \mathbf{b}$  and define for  $i = 2, \dots, 2K$

$$\sigma_i(v) := \begin{cases} \mathbf{b}(v) & \text{if } v \in r_1, \dots, r_{i-1}, \\ 0 & \text{if } v \in r_i \cap (\Lambda_{\mathbf{a}} \cup \Lambda_{\mathbf{c}}), \\ \sigma(v) & \text{if } v \in r_i \cap \Lambda_{\mathbf{b}} \text{ or } v \in r_{i+1}, \dots, r_{2K-1}. \end{cases}$$

In the following description of the procedure the row indices should be taken modulo  $2K$  in view of the periodic boundary conditions. We now describe in detail how to construct each of the paths  $\omega^{(i)}$  for  $i = 1, \dots, 2K$ . Each path  $\omega^{(i)} = (\omega_1^{(i)}, \dots, \omega_{2L+1}^{(i)})$  comprises  $2L + 1$  moves (but possibly void) and is such that  $\omega_1^{(i)} = \sigma_i$  and  $\omega_{2L+1}^{(i)} = \sigma_{i+1}$ . We start from configuration  $\omega_0^{(i)} = \sigma_i$  and we repeat iteratively the following procedure for all  $j = 1, \dots, 2L$ :

- If  $j \equiv 1 \pmod{2}$ , consider the pair of sites  $v \in \Lambda_{\mathbf{a}}$  and  $v' \in \Lambda_{\mathbf{c}}$  defined by

$$\begin{cases} v = (i+1, 3j), & v' = (i+1, 3j+2) & \text{if } i \equiv 0 \pmod{2}, \\ v = (i+1, 3j-3), & v' = (i+1, 3j-1) & \text{if } i \equiv 1 \pmod{2}. \end{cases}$$

Note that the two sites  $v$  and  $v'$  are always neighbors, so that only one of the two can be occupied.

- If  $\omega_j^{(i)}(v) = 0 = \omega_j^{(i)}(v')$ , we set  $\omega_{j+1}^{(i)} = \omega_j^{(i)}$ , so  $H(\omega_{j+1}^{(i)}) = H(\omega_j^{(i)})$ .
- If  $\omega_j^{(i)}(v) = 1$  or  $\omega_j^{(i)}(v') = 1$ , then we remove from configuration  $\omega_j^{(i)}$  the particle in the unique occupied site between  $v$  and  $v'$ , increasing the energy by 1 and obtaining in this way configuration  $\omega_{j+1}^{(i)}$ , which is such that  $H(\omega_{j+1}^{(i)}) = H(\omega_j^{(i)}) + 1$ .
- If  $j \equiv 0 \pmod{2}$ , consider the site  $v \in \Lambda_{\mathbf{b}}$  defined as

$$v = \begin{cases} (i, 3j-2) & \text{if } i \equiv 0 \pmod{2}, \\ (i, 3j-5) & \text{if } i \equiv 1 \pmod{2}. \end{cases}$$

- If  $\omega_j^{(i)}(v) = 1$ , we set  $\omega_{j+1}^{(i)} = \omega_j^{(i)}$  and thus  $H(\omega_{j+1}^{(i)}) = H(\omega_j^{(i)})$ .
- If  $\omega_j^{(i)}(v) = 0$ , then we add to configuration  $\omega_j^{(i)}$  a particle in site  $v$  decreasing the energy by 1. We obtain in this way a configuration  $\omega_{j+1}^{(i)}$ , which is a hard-core configuration because by construction all the first neighboring sites of  $v$  are unoccupied. In particular, the two particles residing in the two sites above  $v$  may have been removed exactly at the previous step. The new configuration has energy  $H(\omega_{j+1}^{(i)}) = H(\omega_j^{(i)}) - 1$ .

The way the path  $\omega^{(i)}$  is constructed shows that for every  $i = 1, \dots, 2K$ ,

$$H(\sigma_{i+1}) \leq H(\sigma_i),$$

since the number of particles added in row  $r_i$  is greater than or equal to the number of particles removed in row  $r_{i+1}$ . Moreover,

$$\Phi_{\omega^{(i)}} \leq H(\sigma_i) + 1$$

since along the path  $\omega^{(i)}$  every particle removal (if any) is always followed by a particle addition. These two properties imply that the path  $\omega : \sigma \rightarrow \mathbf{b}$  created by concatenating  $\omega^{(1)}, \dots, \omega^{(2K)}$  satisfies

$$\Phi_{\omega} \leq H(\sigma) + 1.$$

Note that the energy reduction algorithm by rows can be tweaked in order to have either  $\mathbf{a}$  or  $\mathbf{c}$  as target configuration. In particular, the condition (31) for the initial configuration  $\sigma$  should be adjusted accordingly, requiring that  $\sigma$  has no black and white (black and gray, respectively) particles in the first horizontal stripe  $S_0$ , depending on whether the target configuration is  $\mathbf{a}$  or  $\mathbf{c}$ , respectively.

### Energy reduction algorithm by columns

We now illustrate how the energy reduction algorithm by columns works choosing  $\mathbf{b}$  as target configuration. Note that the procedure we are about to describe can be tweaked to yield a path with target configuration  $\mathbf{a}$  or  $\mathbf{c}$ , but we omit the details. If the target configuration is  $\mathbf{b}$ , we require that the initial configuration  $\sigma \in \mathcal{X}$  has no particles on columns  $c_2$  and  $c_3$ , namely

$$\sigma(v) = 0 \quad \forall v \in c_2 \cup c_3. \quad (32)$$

Since  $c_2 = C_0 \cap \Lambda_{\mathbf{c}}$  and  $c_3 = C_1 \cap \Lambda_{\mathbf{a}}$ , condition (32) requires there are no white particles in  $C_0$  and no gray particles in  $C_1$ . Figure 12 shows a hard-core configuration that satisfies this initial condition.



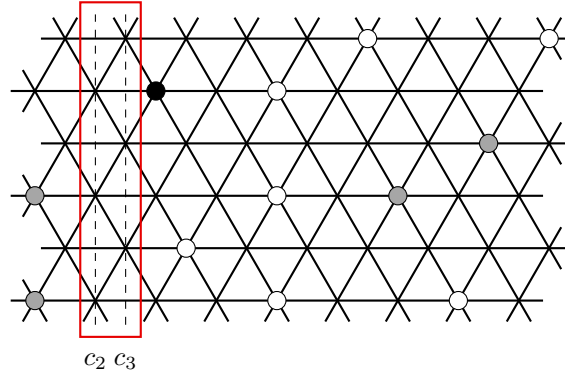


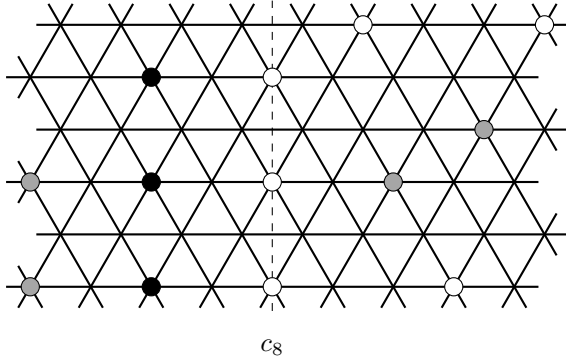
Figure 12: Example of hard-core configuration on the  $6 \times 9$  triangular grid that satisfies (32)

The output of this algorithm is a path  $\omega$  from  $\sigma$  to  $\mathbf{b}$ , which we construct as concatenation of  $2L$  paths  $\omega^{(1)}, \dots, \omega^{(2L)}$ . For every  $j = 1, \dots, 2L$ , path  $\omega^{(j)}$  goes from  $\sigma_j$  to  $\sigma_{j+1}$ , where we set  $\sigma_1 := \sigma$ ,  $\sigma_{2L+1} := \mathbf{b}$  and define for  $j = 2, \dots, 2L$

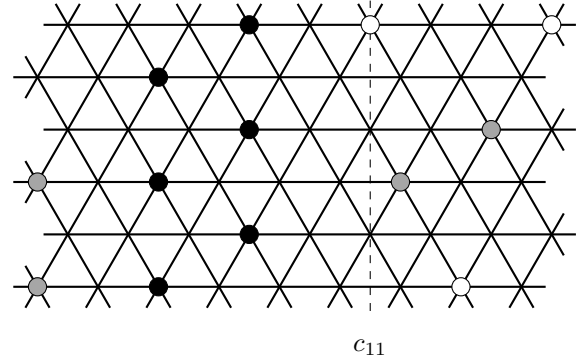
$$\sigma_j(v) := \begin{cases} \mathbf{b}(v) & \text{if } v \in c_2, \dots, c_{3j}, \\ \sigma(v) & \text{if } v \in c_{3j+1}, \dots, c_{6L+1}. \end{cases}$$

The column indices should of course be taken modulo  $6L$ , in view of the periodic boundary conditions. We now describe in detail how to construct each of the paths  $\omega^{(j)}$  for  $j = 1, \dots, 2L$ . We remark that in the procedures we will now describe, also the row index has to be taken modulo  $2K$ .

We distinguish two cases, depending on whether (a)  $\sigma_j$  has a vertical bridge in column  $c_{3j+2}$  or (b) not, see the two examples in Figure 13.



(a) The configuration  $\sigma_1$  has a white bridge on column  $c_8$



(b) The configuration  $\sigma_2$  has no white bridges on column  $c_{11}$

Figure 13: The configurations  $\sigma_1$  and  $\sigma_2$  corresponding to the initial configuration  $\sigma$  in Figure 12

Consider case (a) first. First notice that the presence of a vertical (white) bridge in column  $c_{3j+2}$  implies that all sites of the adjacent column  $c_{3j+3}$  must be empty in configuration  $\sigma_j$ .

We construct a path  $\omega^{(j)} = (\omega_1^{(j)}, \dots, \omega_{2K+1}^{(j)})$  of length  $2K + 1$  (but possibly comprising void moves), with  $\omega_1^{(j)} = \sigma_j$  and  $\omega_{2K+1}^{(j)} = \sigma_{j+1}$ . Denote by  $o(j) \in \{0, 1\}$  the integer number such that  $o(j) \equiv j \pmod{2}$ . We first remove the two white particles in column  $c_{3j+2}$  that lie in row  $r_{o(j)}$  and  $r_{o(j)+2}$  in two successive steps, obtaining in this way configuration  $\omega_3^{(j)}$ , which is such that  $H(\omega_3^{(j)}) = H(\omega_1^{(j)}) + 2$ . We then repeat iteratively the following procedure to obtain the configuration  $\omega_{i+1}^{(j)}$  from  $\omega_i^{(j)}$  for all  $i = 3, \dots, 2K - 1$ :

- If  $i \equiv 1 \pmod{2}$ , consider the site  $v \in c_{3j+1} \subset \Lambda_{\mathbf{b}}$  with coordinates  $(3j+1, o(j) + i - 2)$  and add a (black) particle there, obtaining in this way configuration  $\omega_{i+1}^{(j)}$ . Such a particle can be added since all its six neighboring sites are empty. More specifically, the three left ones have been (possibly) emptied along the path  $\omega^{(j-1)}$ , while the one in  $c_{3j+3}$  is empty by assumption and the other two sites on its right have been emptied in the previous steps of  $\omega^{(j)}$ . Since we added one particle,  $H(\omega_{i+1}^{(j)}) = H(\omega_i^{(j)}) - 1$ .
- If  $i \equiv 0 \pmod{2}$ , consider the site  $v \in c_{3j+2} \subset \Lambda_{\mathbf{c}}$  with coordinates  $(3j+2, o(j) + i)$  and remove the (white) particle lying there, obtaining in this way configuration  $\omega_{i+1}^{(j)}$ , which is such that  $H(\omega_{i+1}^{(j)}) = H(\omega_i^{(j)}) + 1$ .

This procedure outputs configuration  $\omega_{2K}^{(j)}$  which has no white particles in column  $c_{3j+2}$  and an empty site in column  $c_{3j+1}$ , the one with coordinates  $(3j+1, 2K-1-o(j))$ . All the neighboring sites of this site are empty by construction and, adding a black particle in this site, we obtain configuration  $\omega_{2K+1}^{(j)} = \sigma_{j+1}$ , which is such that  $H(\sigma_{j+1}) = H(\omega_{2K}^{(j)}) - 1$ . The way the path  $\omega^{(j)}$  is constructed shows that

$$H(\sigma_{j+1}) = H(\sigma_j),$$

since we added exactly  $K$  (black) particles in column  $c_{3j+1}$  and removed exactly  $K$  (white) particles in columns  $c_{3j+2}$ . Moreover,

$$\Phi_{\omega^{(j)}} = \max_{\eta \in \omega^{(j)}} H(\eta) = H(\sigma_j) + 2 \quad (33)$$

since along the path  $\omega^{(j)}$  every particle removal is followed by a particle addition, except at the beginning when we remove two particles consecutively.

Consider now case (b). We claim that, since there is no vertical (white) bridge in column  $c_{3j+2}$ , there exists a site  $v^*$  in column  $c_{3j+1}$  with at most one neighboring occupied site. First of all, all sites in column  $c_{3j}$  and  $c_{3j-1}$  have been emptied along the path  $\omega^{(j-1)}$ , so all sites in  $c_{3j+1}$  have no left neighboring sites occupied. Let us look now at the right neighboring sites. Since there is no vertical white bridge in column  $c_{3j+2}$ , there exists an empty site in it, say  $w$ . Modulo relabeling the rows, we may assume that  $w$  has coordinates  $(3j+2, o(j))$ , where  $o(j)$  is the integer in  $\{0, 1\}$  such that  $o(j) \equiv j \pmod{2}$ . The site  $v^* = (3j+1, o(j)+1)$  has then the desired property, since at most one of its two remaining right neighboring sites (those with coordinates  $(3j+2, o(j)+2)$  and  $(3j+3, o(j)+1)$ , respectively) can be occupied, since they are also neighbors of each other.

We construct a path  $\omega^{(j)} = (\omega_1^{(j)}, \dots, \omega_{2K+1}^{(j)})$  of length  $2K+1$  (but possibly comprising void moves), with  $\omega_1^{(j)} = \sigma_j$  and  $\omega_{2K+1}^{(j)} = \sigma_{j+1}$ . We then repeat iteratively the following procedure to obtain configuration  $\omega_{i+1}^{(j)}$  from  $\omega_i^{(j)}$  for all  $i = 1, \dots, 2K$ :

- If  $i \equiv 1 \pmod{2}$ , consider the two sites  $(3j+2, o(j)+i+1) \in \Lambda_{\mathbf{c}}$  and  $(3j+3, o(j)+i) \in \Lambda_{\mathbf{a}}$ . Since they are neighboring sites, at most one of them is occupied. If they are both empty, we set  $\omega_{i+1}^{(j)} = \omega_i^{(j)}$ . If instead there is a particle in either of the two, we remove it, obtaining in this way configuration  $\omega_{i+1}^{(j)}$ , which is such that  $H(\omega_{i+1}^{(j)}) = H(\omega_i^{(j)}) + 1$ .
- If  $i \equiv 0 \pmod{2}$ , consider the site  $v \in c_{3j+1} \subset \Lambda_{\mathbf{b}}$  with coordinates  $(3j+1, o(j)+i-1)$  and add a (black) particle there, obtaining in this way configuration  $\omega_{i+1}^{(j)}$ . Such a particle can be added since all its six neighboring sites are empty. More specifically, the three left ones have been (possibly) emptied along the path  $\omega^{(j-1)}$ , while the other two sites on its right have been emptied in the previous step of  $\omega^{(j)}$ . Since we added one particle,  $H(\omega_{i+1}^{(j)}) = H(\omega_i^{(j)}) - 1$ .

The way the path  $\omega^{(j)}$  is constructed shows that

$$H(\sigma_{j+1}) \leq H(\sigma_j),$$

since the number of (black) particles added in column  $c_{3j+1}$  is greater than or equal to the number of (white or gray) particles removed in columns  $c_{3j+2}$  and  $c_{3j+3}$ . Moreover, along the path  $\omega^{(j)}$  every particle removal (if any) is always followed by a particle addition, and hence

$$\Phi_{\omega^{(j)}} = \max_{\eta \in \omega^{(j)}} H(\eta) \leq H(\sigma_j) + 1. \quad (34)$$

Consider now the path  $\omega : \sigma \rightarrow \mathbf{b}$  created by concatenating  $\omega^{(1)}, \dots, \omega^{(2L)}$ , which are constructed either using the procedure in case (a) or that in case (b). First notice that, regardless of which procedure has been used at step  $j$ , the following inequality always holds for every  $j = 1, \dots, 2L$ :

$$H(\sigma_{j+1}) \leq H(\sigma_j).$$

Using this fact in combination with (33) and (34) shows that the path  $\omega$  always satisfies

$$\Phi_{\omega} \leq H(\sigma) + 2.$$

Furthermore, in the special case in which  $\sigma$  has no vertical white bridges, our procedure considers case (b) for every  $j = 1, \dots, 2L$  and thus, by virtue of (34), the path  $\omega$  satisfies

$$\Phi_{\omega} - H(\sigma) \leq 1.$$

We remark that the stable configuration **a** (or **c**) can also be the target configuration of the energy reduction algorithm by columns. In this scenario, one should adjust the condition (32) on the initial condition accordingly, requiring that  $\sigma$  has no particles in columns  $c_1$  and  $c_2$  (columns  $c_0$  and  $c_1$ , respectively). The offset of rows and columns in the procedures described above should of course be tweaked appropriately.

We now use the energy reduction algorithms we just introduced to show that the lower bound for the communication height between **a** and **b** given in Proposition 5.4 is sharp, by explicitly giving a path that attains that value.

**Proposition 5.5** (Reference path). *In the energy landscape corresponding to the hard-core model on the  $2K \times 3L$  triangular grid there exists a path  $\omega^* : \mathbf{a} \rightarrow \mathbf{b}$  in  $\mathcal{X}$  such that*

$$\Phi_{\omega^*} - H(\mathbf{a}) = \min\{K, 2L\} + 1.$$

*Proof.* We distinguish two cases, depending on whether (a)  $K \leq 2L$  and (b)  $K > 2L$ .

For case (a), we construct such a path  $\omega^*$  as the concatenation of two shorter paths,  $\omega^{(1)}$  and  $\omega^{(2)}$ , where  $\omega^{(1)} : \mathbf{a} \rightarrow \sigma^*$  and  $\omega^{(2)} : \sigma^* \rightarrow \mathbf{b}$  for a suitable configuration  $\sigma^* \in \mathcal{X}$ , and prove that  $\Phi_{\omega^{(1)}} = H(\sigma^*) = H(\mathbf{a}) + K$  and that  $\Phi_{\omega^{(2)}} = H(\sigma^*) + 1$  are satisfied, so that  $\Phi_{\omega^*} = H(\mathbf{a}) + K + 1$  as desired. The reason why  $\omega$  is best described as the concatenation of two shorter paths is the following: The energy reduction algorithm by columns cannot in general be started directly from **a** and the path  $\omega^{(1)}$  indeed leads from **a** to  $\sigma^*$ , which is a suitable configuration to initialize the energy reduction algorithm by columns. The configuration  $\sigma^*$  differs from **a** only in the sites of column  $c_3$ :

$$\sigma^*(v) := \begin{cases} \mathbf{a}(v) & \text{if } v \in \Lambda \setminus c_3, \\ 0 & \text{if } v \in c_3. \end{cases}$$

The path  $\omega^{(1)} = (\omega_1^{(1)}, \dots, \omega_{K+1}^{(1)})$ , with  $\omega_1^{(1)} = \mathbf{a}$  and  $\omega_{K+1}^{(1)} = \sigma^*$  can be constructed as follows. For  $i = 1, \dots, K$ , at step  $i$  we remove from configuration  $\omega_i^{(1)}$  the particle in the site of coordinates  $(3, 2i - 1)$ , increasing the energy by 1 and obtaining in this way configuration  $\omega_{i+1}^{(1)}$ . Therefore the configuration  $\sigma^*$  is such that  $H(\sigma^*) - H(\mathbf{a}) = K$  and  $\Phi_{\omega^{(1)}} = H(\mathbf{a}) + K$ .

The second path  $\omega^{(2)} : \sigma^* \rightarrow \mathbf{b}$  is then constructed by means of the energy reduction algorithm by columns, which can be used since the configuration  $\sigma^*$  satisfies condition (32) and hence is a suitable initial configuration for the algorithm. Since configuration  $\sigma^*$  has no vertical white bridges (see case (b) for the energy reduction algorithm by columns), the procedure guarantees that

$$\Phi_{\omega^{(2)}} = H(\sigma^*) + 1 = H(\mathbf{a}) + K + 1,$$

and thus the conclusion follows. Figure 14 illustrates the reference path for the  $6 \times 9$  triangular grid.

For case (b), we construct such a path  $\omega^*$  as the concatenation of two shorter paths,  $\omega^{(1)}$  and  $\omega^{(2)}$ , where  $\omega^{(1)} : \mathbf{a} \rightarrow \sigma^*$  and  $\omega^{(2)} : \sigma^* \rightarrow \mathbf{b}$ , and prove that  $\Phi_{\omega^{(1)}} = H(\sigma^*) = H(\mathbf{a}) + 2L$  and that  $\Phi_{\omega^{(2)}} = H(\sigma^*) + 1$  are satisfied, so that  $\Phi_{\omega^*} = H(\mathbf{a}) + 2L + 1$  as desired. Some snapshots from the reference path from **a** to **b** on the  $10 \times 6$  triangular grid are presented in Figure 15. Also in this case we construct  $\omega$  as concatenation of two shorter paths because **a** is not a suitable initial configuration for a energy reduction algorithm. Consider the configuration  $\sigma^*$  that differs from **a** only in the sites of the first horizontal stripe  $S_0$ , namely

$$\sigma^*(v) := \begin{cases} \mathbf{a}(v) & \text{if } v \in \Lambda \setminus S_0, \\ 0 & \text{if } v \in S_0. \end{cases}$$

The path  $\omega^{(1)} = (\omega_1^{(1)}, \dots, \omega_{2L+1}^{(1)})$ , with  $\omega_1^{(1)} = \mathbf{a}$  and  $\omega_{2L+1}^{(1)} = \sigma^*$  can be constructed as follows. For  $i = 1, \dots, 2L$ , at step  $i$  we remove from configuration  $\omega_i^{(1)}$  the first particle in lexicographic order in  $S_0$ , increasing the energy by 1 and obtaining in this way configuration  $\omega_{i+1}^{(1)}$ . Therefore the configuration  $\sigma^*$  is such that  $H(\sigma^*) - H(\mathbf{a}) = 2L$  and  $\Phi_{\omega^{(1)}} = H(\mathbf{a}) + 2L$ .

The second path  $\omega^{(2)} : \sigma^* \rightarrow \mathbf{b}$  is then constructed by means of the energy reduction algorithm by rows, which can be used since the configuration  $\sigma^*$  satisfies condition (31) and hence is a suitable initial configuration for the algorithm. The energy reduction algorithm by rows guarantees that

$$\Phi_{\omega^{(2)}} = H(\sigma^*) + 1 = H(\mathbf{a}) + 2L + 1.$$

and thus the conclusion follows.  $\square$

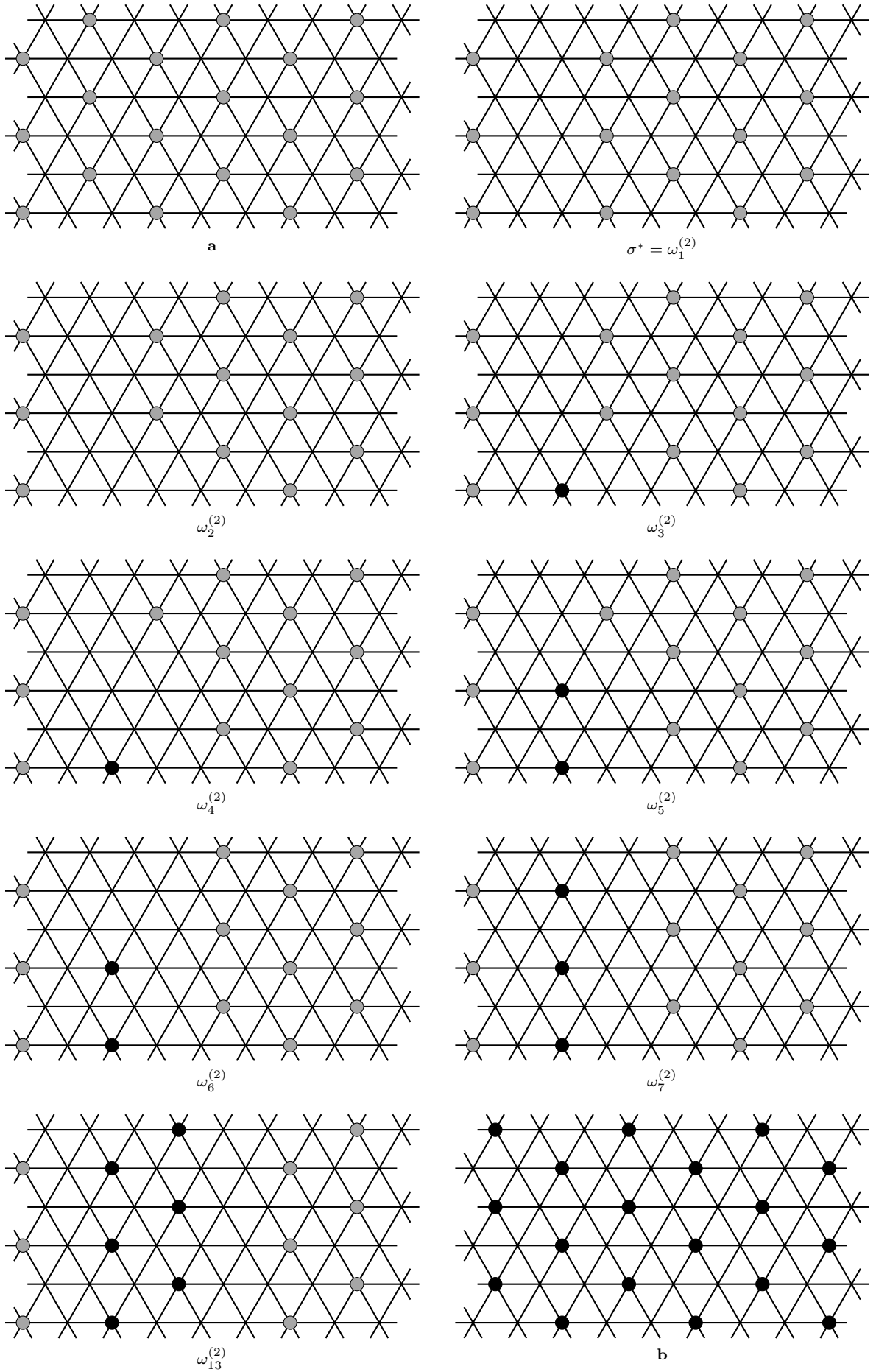


Figure 14: Illustration of the reference path  $\omega^* : \mathbf{a} \rightarrow \mathbf{b}$  in the case  $K \leq 2L$

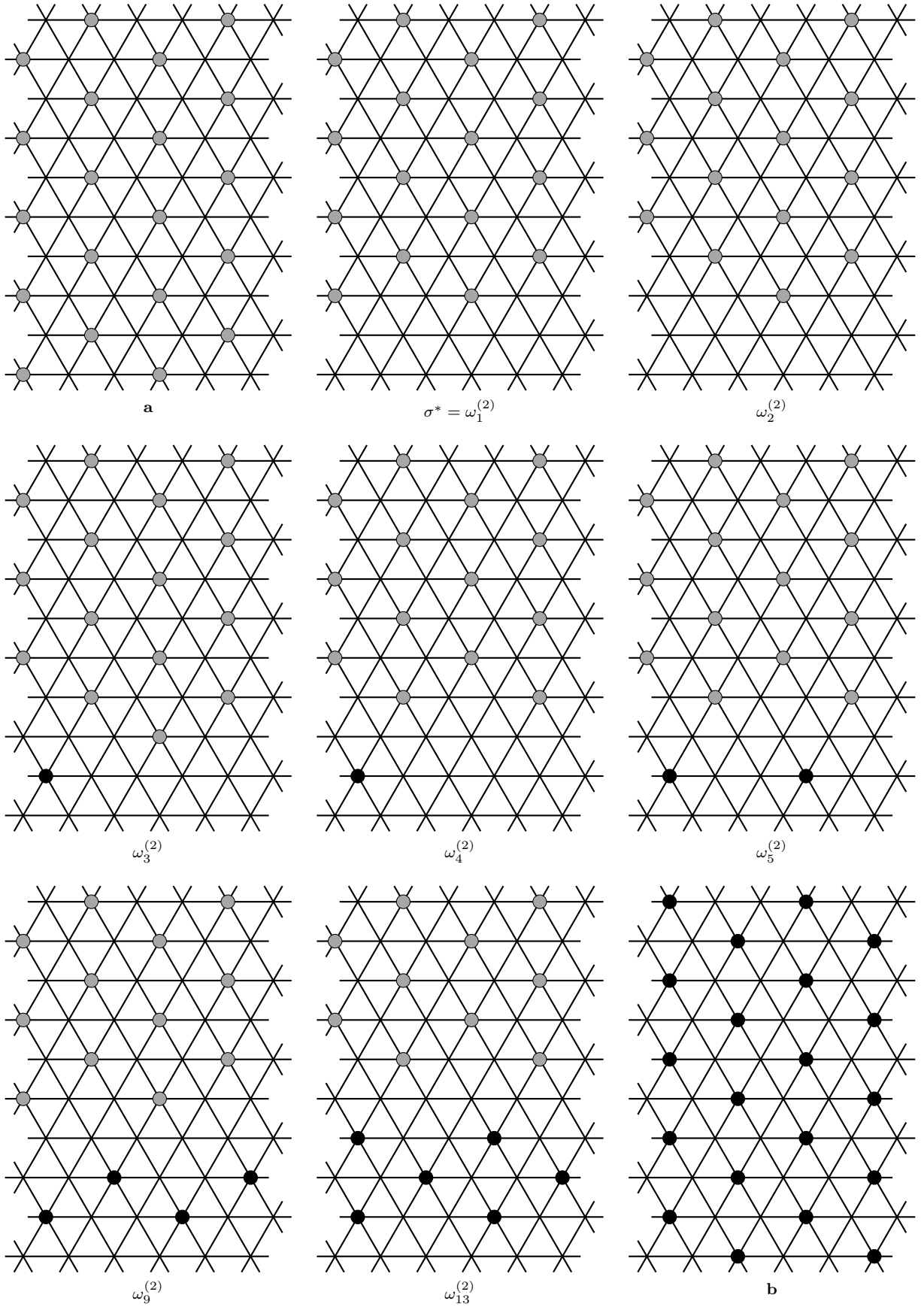


Figure 15: Illustration of the reference path  $\omega^* : \mathbf{a} \rightarrow \mathbf{b}$  in the case  $K > 2L$



*Proof of Theorem 3.1(ii).* The proof of the identity involving  $\Phi(\mathbf{a}, \mathbf{b}) - H(\mathbf{a})$  readily follows by combining the lower bound in Proposition 5.4 and the statement of Proposition 5.5; the remaining identities immediately follow from symmetry of the triangular grid.  $\square$

*Proof of Theorem 3.1(iii).* We will show that for every hard-core configuration  $\sigma$  on the  $2K \times 3L$  triangular grid with  $\sigma \neq \mathbf{a}, \mathbf{b}, \mathbf{c}$ , there exists a path  $\omega$  from  $\sigma$  to one of the three stable configurations such that

$$\Phi_\omega - H(\sigma) \leq \min\{K, 2L\}.$$

The idea is to construct such a path using the geometric features of the configuration  $\sigma$  and exploiting the energy reduction algorithms described earlier in this section. We start by distinguishing two cases: (a)  $K \leq 2L$  and (b)  $K > 2L$ .

Consider case (a) first, where  $K \leq 2L$ . We distinguish two sub-cases, depending on whether  $\sigma$  has at least one vertical bridge or not.

If  $\sigma$  has a vertical bridge in a vertical stripe  $C$ , then  $\sigma$  is a suitable starting configuration for the energy reduction algorithm, which yields a path  $\omega$  that goes from  $\sigma$  to the stable configuration in  $\{\mathbf{a}, \mathbf{b}, \mathbf{c}\}$  on which  $\sigma$  agrees in stripe  $C$ . The path  $\omega$  constructed in this way is such that  $\Phi_\omega - H(\sigma) \leq 2$  and thus  $\Phi(\sigma, \{\mathbf{a}, \mathbf{b}, \mathbf{c}\}) - H(\sigma) \leq 2 \leq K \leq \min\{K, 2L\}$ , since by assumption  $K$  is an integer greater than 1.

Suppose now that there are no vertical bridges in  $\sigma$ . Since  $\sigma \notin \{\mathbf{a}, \mathbf{b}, \mathbf{c}\}$ , which is the set of stable configurations in view of Theorem 3.1(i), configuration  $\sigma$  has a positive energy difference  $\Delta H(\sigma) > 0$ . In view of (22), this means that there exists a vertical stripe  $C^*$  such that  $\Delta H_{C^*}(\sigma) > 0$ . Without loss of generality, we may assume (modulo relabeling) that  $C^*$  is the vertical stripe  $C_1$ , which consists of columns  $c_1, c_2$  and  $c_3$ . By definition of energy difference in a stripe, it follows that  $\sigma$  has at most  $K - 1$  particles. Removing all the gray and white particles one by one, we construct a path  $\omega^{(1)}$  from  $\sigma$  to a new configuration  $\sigma^*$  defined as

$$\sigma^*(v) := \begin{cases} \sigma(v) & \text{if } v \in \Lambda \setminus (c_2 \cup c_3), \\ 0 & \text{if } v \in c_2 \cup c_3. \end{cases}$$

Since  $\sigma$  has at most  $K - 1$  particles in the vertical stripe  $C_1$ , it follows that

$$H(\sigma^*) - H(\sigma) \leq K - 1 \quad \text{and} \quad \Phi_{\omega^{(1)}} - H(\sigma) \leq K - 1. \quad (35)$$

Since we remove all the gray particles from  $c_3$  and all the white particles from  $c_2$ ,  $\sigma^*$  is a suitable starting configuration for the energy reduction algorithm by columns with target configuration  $\mathbf{b}$ , in view of (32). We obtain in this way a second path  $\omega^{(2)} : \sigma^* \rightarrow \mathbf{b}$ , which is such that

$$\Phi_{\omega^{(2)}} - H(\sigma^*) \leq 1, \quad (36)$$

thanks to the absence of vertical bridges in  $\sigma$  (and thus in  $\sigma^*$ ). In view of (35) and (36), the path  $\omega : \sigma \rightarrow \mathbf{b}$  obtained by concatenating  $\omega^{(1)}$  and  $\omega^{(2)}$  is such that

$$\Phi_\omega - H(\sigma) \leq K,$$

and hence  $\Phi(\sigma, \{\mathbf{a}, \mathbf{b}, \mathbf{c}\}) - H(\sigma) \leq K$ .

We remark that there is nothing special about  $\mathbf{b}$  as target configuration of the path  $\omega$  we just constructed. Indeed, by choosing the vertical stripe  $C^*$  with a different offset, we could have obtained a configuration  $\sigma^*$  which would have been a suitable initial configuration for the energy reduction algorithm by columns with target configuration  $\mathbf{a}$  or  $\mathbf{c}$ .

We now turn to case (b), in which  $K > 2L$ . Thanks to Lemma 5.2, there must be a horizontal stripe  $S$  on which  $\sigma$  does not have a horizontal bridge, otherwise  $\sigma \in \{\mathbf{a}, \mathbf{b}, \mathbf{c}\}$ . In particular,  $\sigma$  has at most  $2L - 1$  particles on  $S$ , which without loss of generality we may assume to be  $S_0$ . We construct a path  $\omega^{(1)}$  from  $\sigma$  to a new configuration  $\sigma^*$  by removing all these particles one by one, so that  $\Phi_{\omega^{(1)}} - H(\sigma) \leq 2L - 1$  and  $H(\sigma^*) - H(\sigma) \leq 2L - 1$ . Starting with configuration  $\sigma^*$  we can then use the energy reduction algorithm by rows to obtain a second path  $\omega^{(2)}$  from  $\sigma^*$  to any of the three stable configurations. Since  $\Phi_{\omega^{(2)}} - H(\sigma^*) \leq 1$ , the path  $\omega$  constructed by the concatenation of  $\omega^{(1)}$  and  $\omega^{(2)}$  satisfies

$$\Phi_\omega - H(\sigma) \leq 2L$$

and thus  $\Phi(\sigma, \{\mathbf{a}, \mathbf{b}, \mathbf{c}\}) - H(\sigma) \leq 2L$ .  $\square$

**Acknowledgments** The author is supported by NWO grant 639.033.413. The author is grateful to F.R. Nardi, S.C. Borst, and J.S.H. van Leeuwen for the precious feedback and helpful discussions related to this work.

## References

- [1] G.E. Andrews. The hard-hexagon model and Rogers-Ramanujan type identities. *Proceedings of the National Academy of Sciences of the United States of America*, 78(9):5290–5292, 1981.
- [2] R.J. Baxter. Hard hexagons: Exact solution. *Journal of Physics A: Mathematical and General*, 13(3):L61–L70, 1999.
- [3] R.J. Baxter, I.G. Enting, and S.K. Tsang. Hard-square lattice gas. *Journal of Statistical Physics*, 22(4):465–489, 1980.
- [4] J. Beltrán and C. Landim. Tunneling of the Kawasaki dynamics at low temperatures in two dimensions. *Annales de l’Institut Henri Poincaré, Probabilités et Statistiques*, 51(1):59–88, 2015.
- [5] A. Blanca, Y. Chen, D. Galvin, D. Randall, and P. Tetali. Phase Coexistence for the Hard-Core Model on  $\mathbb{Z}^2$ . *Preprint at arXiv:1611.01115*, 2016.
- [6] A. Blanca, D. Galvin, D. Randall, and P. Tetali. Phase coexistence and slow mixing for the hard-core model on  $\mathbb{Z}^2$ . In *Approximation, Randomization, and Combinatorial Optimization. Algorithms and Techniques*, volume 8096 of *Lecture Notes in Computer Science*, pages 379–394. Springer, Berlin, Heidelberg, 2013.
- [7] C. Borgs, J.T. Chayes, A. Frieze, P. Tetali, E. Vigoda, and H.V. Van. Torpid mixing of some Monte Carlo Markov chain algorithms in statistical physics. In *Foundations of Computer Science, 1999. 40th Annual Symposium on*, pages 218–229, 1999.
- [8] M. Cassandro, A. Galves, E. Olivieri, and M.E. Vares. Metastable behavior of stochastic dynamics: A pathwise approach. *Journal of Statistical Physics*, 35(5-6):603–634, 1984.
- [9] O. Catoni. Simulated annealing algorithms and Markov chains with rare transitions. In *Séminaire de probabilités XXXIII*, volume 1709 of *Lecture Notes in Mathematics*, pages 69–119. Springer Berlin, 1999.
- [10] E.N.M. Cirillo and F.R. Nardi. Metastability for a stochastic dynamics with a parallel heat bath updating rule. *Journal of Statistical Physics*, 110(1-2):183–217, 2003.
- [11] E.N.M. Cirillo and F.R. Nardi. Relaxation height in energy landscapes: An application to multiple metastable states. *Journal of Statistical Physics*, 150(6):1080–1114, 2013.
- [12] F. den Hollander, F.R. Nardi, E. Olivieri, and E. Scoppola. Droplet growth for three-dimensional Kawasaki dynamics. *Probability Theory and Related Fields*, 125(2):153–194, 2003.
- [13] F. den Hollander, E. Olivieri, and E. Scoppola. Metastability and nucleation for conservative dynamics. *Journal of Mathematical Physics*, 41(3):1424, 2000.
- [14] R.L. Dobrushin. The problem of uniqueness of a gibbsian random field and the problem of phase transitions. *Functional Analysis and Its Applications*, 2(4):302–312, 1969.
- [15] M. Durvy, O. Dousse, and P. Thiran. Border effects, fairness, and phase transition in large wireless networks. In *INFOCOM, 2008 Proceedings*, pages 601–609. IEEE, 2008.
- [16] M. Dyer, A. Frieze, and M. Jerrum. On counting independent sets in sparse graphs. *SIAM Journal on Computing*, 31(5):1527–1541, 2002.
- [17] D. Galvin. Sampling independent sets in the discrete torus. *Random Structures and Algorithms*, 33(3):356–376, 2008.
- [18] D. Galvin and J. Kahn. On Phase Transition in the Hard-Core Model on  $\mathbb{Z}^d$ . *Combinatorics, Probability and Computing*, 13(2):137–164, 2004.
- [19] D. Galvin, F. Martinelli, K. Ramanan, and P. Tetali. The Multistate Hard Core Model on a Regular Tree. *SIAM Journal on Discrete Mathematics*, 25(2):894–915, 2011.
- [20] D. Galvin and P. Tetali. Slow mixing of Glauber dynamics for the hard-core model on the hypercube. *Proceedings of SODA ’04*, pages 466–467, 2004.
- [21] D. Galvin and P. Tetali. Slow mixing of Glauber dynamics for the hard-core model on regular bipartite graphs. *Random Structures and Algorithms*, 28(4):427–443, 2006.
- [22] D.S. Gaunt. Hard-Sphere Lattice Gases. II. Plane-Triangular and Three-Dimensional Lattices. *The Journal of Chemical Physics*, 46(8):3237–3259, 1967.

- [23] D.S. Gaunt and M.E. Fisher. Hard-Sphere Lattice Gases. I. Plane-Square Lattice. *The Journal of Chemical Physics*, 43(8):2840, 1965.
- [24] S. Greenberg and D. Randall. Slow mixing of Markov chains using fault lines and fat contours. *Algorithmica*, 58(4):911–927, 2010.
- [25] O.J. Heilmann and E. Praestgaard. Phase transition of hard hexagons on a triangular lattice. *Journal of Statistical Physics*, 9(1):23–44, 1973.
- [26] F.P. Kelly. Stochastic models of computer communication systems. *Journal of the Royal Statistical Society. Series B*, 47(3):379–395, 1985.
- [27] R. Kotecký and E. Olivieri. Droplet dynamics for asymmetric Ising model. *Journal of Statistical Physics*, 70(5-6):1121–1148, 1993.
- [28] C. Landim and P. Lemire. Metastability of the Two-Dimensional Blume-Capel Model with Zero Chemical Potential and Small Magnetic Field. *Journal of Statistical Physics*, 164(2):346–376, 2016.
- [29] C. Landim and I. Seo. Metastability of Non-reversible, Mean-Field Potts Model with Three Spins. *Journal of Statistical Physics*, 165(4):693–726, 2016.
- [30] D.A. Levin, Y. Peres, and E. Wilmer. *Markov Chains and Mixing Times*. AMS, Providence, Rhode Island, 2009.
- [31] M. Luby and E. Vigoda. Fast convergence of the Glauber dynamics for sampling independent sets. *Random Structures and Algorithms*, 1198(92):229–241, 1999.
- [32] B. Luen, K. Ramanan, and I. Ziedins. Nonmonotonicity of phase transitions in a loss network with controls. *The Annals of Applied Probability*, 16(3):1528–1562, 2006.
- [33] F. Manzo, F.R. Nardi, E. Olivieri, and E. Scoppola. On the essential features of metastability: Tunnelling time and critical configurations. *Journal of Statistical Physics*, 115(1/2):591–642, 2004.
- [34] L. Miclo. About relaxation time of finite generalized Metropolis algorithms. *The Annals of Applied Probability*, 12(4):1492–1515, 2002.
- [35] E. Mossel, D. Weitz, and N.C. Wormald. On the hardness of sampling independent sets beyond the tree threshold. *Probability Theory and Related Fields*, 143(3-4):401–439, 2008.
- [36] F.R. Nardi, E. Olivieri, and E. Scoppola. Anisotropy effects in nucleation for conservative dynamics. *Journal of Statistical Physics*, 119(3-4):539–595, 2005.
- [37] F.R. Nardi, A. Zocca, and S.C. Borst. Hitting Time Asymptotics for Hard-Core Interactions on Grids. *Journal of Statistical Physics*, 162(2):522–576, 2016.
- [38] E.J. Neves and R.H. Schonmann. Critical droplets and metastability for a Glauber dynamics at very low temperatures. *Communications in Mathematical Physics*, 137(2):209–230, 1991.
- [39] R. Peled and W. Samotij. Odd cutsets and the hard-core model on  $\mathbb{Z}^d$ . *Annales de l’Institut Henri Poincaré, Probabilités et Statistiques*, 50(3):975–998, 2014.
- [40] K. Ramanan, A. Sengupta, I. Ziedins, and P. Mitra. Markov random field models of multicasting in tree networks. *Advances in Applied Probability*, 34(1):58–84, 2002.
- [41] D. Randall. Slow mixing of Glauber dynamics via topological obstructions. *Proceedings of SODA ’06*, pages 870–879, 2006.
- [42] R. Restrepo, J. Shin, P. Tetali, E. Vigoda, and Y. Linji. Improved mixing condition on the grid for counting and sampling independent sets. *Probability Theory and Related Fields*, 156(1-2):75–99, 2013.
- [43] L.K. Runnels and L.L. Combs. Exact Finite Method of Lattice Statistics. I. Square and Triangular Lattice Gases of Hard Molecules. *The Journal of Chemical Physics*, 45(7):2482–2492, 1966.
- [44] A. Sinclair, P. Srivastava, D. Štefankovič, and Y. Yin. Spatial mixing and the connective constant: optimal bounds. *Probability Theory and Related Fields*, pages 1–45, 2016.
- [45] F. Spitzer. Markov Random Fields on an Infinite Tree. *The Annals of Probability*, 3(3):387–398, 1975.

- [46] Y.M. Suhov and U.A. Rozikov. A hard-core model on a Cayley tree: An example of a loss network. *Queueing Systems*, 46(1/2):197–212, 2004.
- [47] J. van den Berg and J.E. Steif. Percolation and the hard-core lattice gas model. *Stochastic Processes and their Applications*, 49(2):179–197, 1994.
- [48] J.C. Vera, E. Vigoda, and L. Yang. Improved Bounds on the Phase Transition for the Hard-Core Model in 2 Dimensions. *SIAM Journal on Discrete Mathematics*, 29(4):1895–1915, 2015.
- [49] X. Wang and K. Kar. Throughput modelling and fairness issues in CSMA/CA based ad-hoc networks. In *INFOCOM 2005, Proceedings*, volume 1, pages 23–34. IEEE, 2005.
- [50] Y. Yemini. A statistical mechanics of distributed resource sharing mechanisms. In *INFOCOM, 1983 Proceedings*, pages 531–539. IEEE, 1983.
- [51] A. Zocca, S.C. Borst, and J.S.H. van Leeuwen. Mixing properties of CSMA networks on partite graphs. In *Proceedings of VALUETOOLS 2012*, pages 117–126. IEEE, 2012.
- [52] A. Zocca, S.C. Borst, and J.S.H. van Leeuwen. Slow transitions and starvation in dense random-access networks. *Stochastic Models*, 31(3):361–402, 2015.
- [53] A. Zocca, S.C. Borst, J.S.H. van Leeuwen, and F.R. Nardi. Delay performance in random-access grid networks. *Performance Evaluation*, 70(10):900–915, 2013.